

学位論文 Doctoral Thesis

Analysis of Tsukushi (TSK) function in the central nervous system
(中枢神経系における Tsukushi (TSK) 分子の機能解析)

伊 藤 綾 子
Ayako Ito

熊本大学大学院医学教育部博士課程生体医科学専攻神経分化学

指導教員

田中 英明 教授

熊本大学大学院医学教育部博士課程医学専攻神経分化学分野

2011年3月

Contents

Summary	3-5
List of Abbreviations	5
List of Publications	6
Acknowledgements	7
1. Introduction	8-12
1-1. Literature review	
1-2. Background and Specific Aims	
2. Material and Methods	13-16
2-1. chick embryos	
2-2. In situ hybridization	
2-3. In ovo electroporation	
2-4. Mice	
2-5. Tissue processing	
2-6. Immunohistochemistry	
2-7. Hematoxylin and Kluver-Barrera (KB) staining	
2-8. Antibodies	
2-9. DiI labeling	
3.Results	17-50
3-1: Part A:	17-41
Tsukushi functions as a Wnt signaling inhibitor by binding to Frizzled4 in competition with Wnt2b	
3-1-1. TSK expression in the adult mouse eye	
3-1-2. Loss of TSK results in expansion of CB in vivo	
3-1-3. Effects of TSK on retinal spheres in vitro	

- 3-1-4. Expression of TSK at the peripheral chick retina.
- 3-1-5. TSK inhibits Wnt2b activity in vitro.
- 3-1-6. TSK inhibits Wnt2b activity in vivo.
- 3-1-7. TSK binds to Fzd4 directly.
- 3-1-8. Fzd4 is a TSK receptor

3-2: Part B:

42-51

Tsukushi regulates neural stem/progenitor cell proliferation in the mouse brain.

- 3-2-1. TSK expression in the SVZ
- 3-2-2. TSK loss affects neural stem cell/ progenitor cell proliferation and brain size.
- 3-2-3. Cell death is increased in the SVZ stem cells around P14.
- 3-2-4. TSK deletion led to the expansion of RMS in the aSVZ.

3-3: Part C:

52-60

Tsukushi is required for the anterior commissure formation in mouse brain

- 3-3-1. TSK is expressed in the mouse brain
- 3-3-2. TSK deletion affects the anterior commissure tract
- 3-3-3. TSK is involved in AC formation
- 3-3-4. aAC axons never cross the midline

4. Discussion

61-66

- 4-1: Part A and Part B
- 4-2: Part C

5. Conclusion

67-69

- 5-1: Part A
- 5-2: Part B
- 5-3: Part C
- 5-4: Final conclusion

6. References

70-74

Summary

We previously reported that Tsukushi (TSK) is a short range secreted protein. In early embryogenesis, TSK is involved in neurulation by regulating the pivotal signaling cascades such as BMP, Notch, and FGF. In this study, I investigated the TSK expression pattern in the vertebrate (chick and mouse) retina and the mouse brain. I find that TSK is expressed in the CMZ in the chick and the CB and the SVZ in the mouse eye and brain, where neuronal stem/progenitor cells proliferation and differentiation are controlled by Wnt signaling. TSK functions as Wnt signaling inhibitor at the extracellular region by directly bind to the cysteine rich domain (CRD) of Frizzled-4, where Wnt binds. I perform TSK overexpression into chick retina and find that TSK inhibits Wnt activity in vivo and in vitro. In addition, to address TSK function in vivo, we established TSK^{-/-} mice by inserting a lacZ/Neo cassette into the TSK coding exon. TSK inactivation results in expansion of the adult CB and increased proliferation of the retinal stem/progenitor cells isolated from it. These results indicate that TSK is an important component of the stem/progenitor cells niche in the adult mammalian CB, controlling stem/progenitor cells proliferation by modulating Wnt signaling.

In adult mammalian brain, stem/progenitor cells are located in the SVZ and the SGZ. TSK is strongly expressed in the SVZ and the SGZ from neonate to the adult stages. Neural cell types are well studied in the SVZ. To investigate which cell express TSK, I performed immunohistochemical detection and find the TSK expression in a single layer of ependymal cells lining the ventricular cavity. Cell proliferation in the SVZ of TSK^{-/-} brain is increased comparing to the control mouse. From the eye and the brain data, I propose that TSK regulates the stem/progenitor cells proliferation by modulating the pivotal signaling at the extracellular region.

Furthermore, I find another phenotype in the TSK^{-/-} mouse brain. The anterior commissure (AC) is one of the important commissure projections in the brain that conveys information from one side of the nervous system to the other. During development, the axons from the anterior AC (aAC) and the posterior AC (pAC) course in the same dorsoventral plane and converge into a common fascicle for midline crossing. In mice lacking TSK, the aAC and the pAC axons fail to cross the midline, leading to an almost total absence of the AC in adult mice. DiI labeling indicates that the aAC axons grow out from the anterior olfactory nucleus and migrate along normal pathways but never cross the midline. Therefore, I have uncovered a crucial role of TSK in AC formation in the mouse brain.

From present data, I propose that TSK is a signaling modulator at the extracellular region and controls stem/progenitor cells proliferation and axonal guidance in CNS.

List of Abbreviations

µg:	Microgram
µl :	Microlitel
µm:	Micrometer
mm:	Millimetre
nM:	Nanomolar
mM:	Milimolar
FCS:	Fetal calf serum
DMEM:	Dulbeccos modified eagles medium
β-gal:	Beta-galactosidase
CRD	cysteine rich domain
CB	ciliary body
SLRP	Small Leucine-rich Repeat Proteoglycan/protein
SVZ	subventricular zone
SGZ	subgranular zone
CNS	central nervous system
AC	Anterior commissure
aAC	anterior part of anterior commissure
pAC	posterior part of anterior commissure
AON	Anterior olfactory nucleus
TSK	Tsukushi

List of publications

Ito A., Shinmyo Y., Abe T., Oshima N., Tanaka H., Ohta K.

Tsukushi is required for anterior commissure formation in mouse brain.

Biochemical Biophysical Research Communications 402, 813-818. 2010.

Ohta K., **Ito A.**, Tanaka H.

Neuronal stem/progenitor cells in the vertebrate eye

Dev. Growth Differ. 50(4): 253-259. 2008.

Manuscript under revision

Ohta K [§], **Ito A** [§], Kuriyama S, Lupo G, Kosaka M, Ohnuma S, Nakagawa S, and
Tanaka H

Tsukushi functions as a Wnt signaling inhibitor by competing with Wnt2b for binding to
Frizzled4

[§]Equal contribution

Acknowledgements

I would like to deeply thank the many people who, during the Master and PhD student time, provided me with useful and helpful assistance. Without their care, this thesis would likely not have done.

I take immense pleasure in thanking Professor. Hideaki Tanaka, Associate Prof. Kunimasa Ohta and Assistant Prof. Yohei Shinmyo for having permitted me to carry out this project work.

I am very much grateful to my supervisor Associate Professor Dr. Kunimasa Ohta for giving me the opportunity to do this challenging work under his supervision. I gratefully acknowledge his kindness, guidance and constructive criticism of my research work. He gave me a lot of chance to enjoy the research life.

I am thankful to Ministry of Education, Science, Sports and Culture of Japan (MEXT), the 21st Century COE program, the Global COE program (Cell Fate Regulation Research and Education Unit), Japan and Kumamoto University for financial support.

I would like to thank to our lab secretary Ms. Mitsue Kumamaru, Ms. Mihoko Iimori and Ms. Kumiko Hori for their cooperation in carrying out this project work.

I wish to express my deep sense of gratitude to my beloved Lab mate Dr. Giasuddin Ahmed, Dr. Iftekhhar Bin Naser, Ms. Xiaohong Song, Ms. Athary Fekemban, Mr. Mahmud Hossain, Mr Asrafuzzaman Riyadh, Dr. Shahidul M Islam, Dr. Yuhong Su, Dr. Sanbing Zhang, who discussed my project with me and gave me many suggestion. They gave me wonderful time and a lot of smile.

Finally, I thank to my parents and my sister to the support of my life. This thesis would not have been possible without the complete support of my family.

1. Introduction

1-1. Literature review

1-1-1. TSK is a member of Small Leucine-rich Repeat Proteoglycan/proteins (SLRP) family

A number of gene families of secreted proteins are involved in the regulation of various kind of biological processes: morphogenesis, cellular differentiation, angiogenesis, apoptosis, and modulation of the immune responses. Secreted proteins belong to Small Leucine-rich Repeat Proteoglycan/protein (SLRP) family are evolutionally conserved. SLRP proteins were synthesized as a small core protein containing 6-20 leucine-rich repeat (LRR) motifs and post-translationally modified with glycosaminoglycan (GAG) chain (s), N-glycosylation, and/or tyrosine sulfation. The SLRP gene family has 17 genes. It was classified into five distinct families based on numbers of exons, homology at the protein and the presence of characteristic N-terminal cysteine-rich clusters with defined spacing. Classes I-III is canonical class of SLRP genes. Class I includes decorin, biglycan and asporin; class II includes fibromodulin, osteoadherin, lumican, proline arginine-rich end LRP protein (PRELP), and keratocan; and Class III includes opticin, osteoglycin/mimecan, and epiphycan/PGLb. Classes IV and V are new non-canonical classes of SLRPs (Schaefer et al., 2008) (Figure 1'). SLRP family proteins are involved in several fundamental biological functions. Decorin and biglycan play important roles in regulation of matrix assembly, collagen fibrillogenesis, cellular proliferation, cell differentiation and migration in various tissues (Lozzo, 1999; Schaefer et al., 2008).

We previously reported the identification of a new member of SLRP family, named

Tsukushi, identified by signal sequence trap screening using a chick lens library (Ohta et al., 2004). TSK has 12 LRRs, which are located between the two cysteine clusters at the N and C termini (Figure 2'). In early embryogenesis, TSK is involved in neurulation by regulating pivotal signaling cascades. First, TSK functions as an organizer inducer by inhibiting Bone Morphogenetic Protein (BMP) signaling in cooperation with chordin (Ohta et al., 2004). Second, TSK interacts with Vg1 to induce the primitive streak and the Hensen's node in the chick embryo (Ohta et al., 2006). Third, TSK controls the ectodermal patterning and the neural crest specification in *Xenopus* by direct regulation of BMP4 and the activity of Notch ligand Delta-1 (Kuriyama et al., 2006). Finally, X-TSK modulates *Xnr*, fibroblast growth factor (FGF), and BMP signaling and regulates germ layer formation and patterning in the *Xenopus* embryo (Morris et al., 2007).

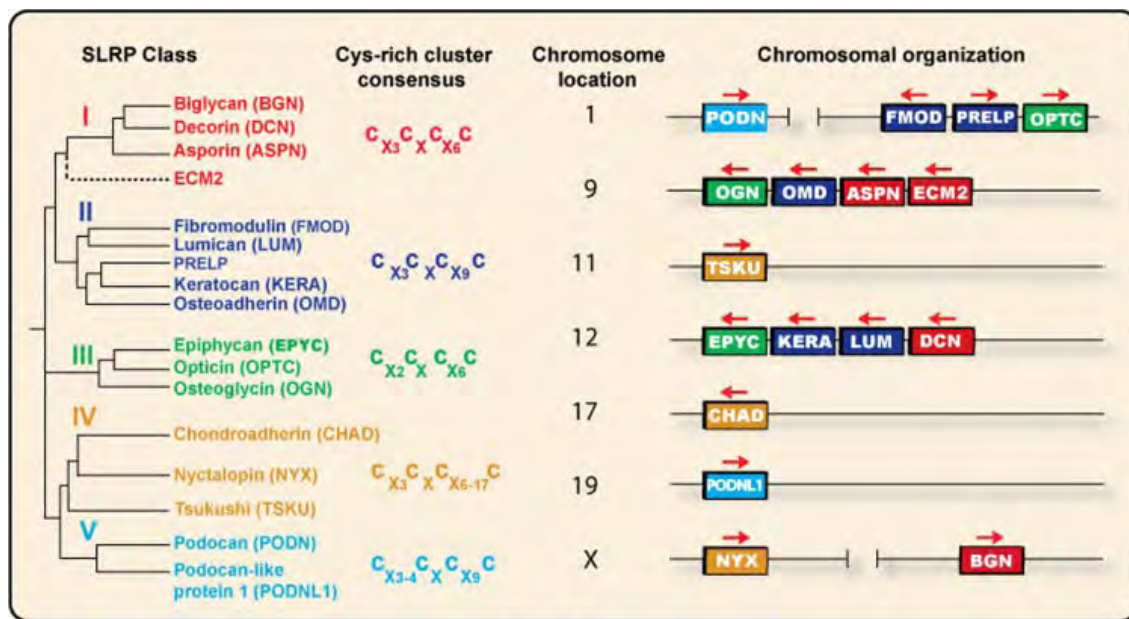


Figure 1'. Phylogenetic analysis and chromosomal organization of various human SLRP classes. The color-coded dendrogram (left) shows the presence of five distinct families of SLRP and related LRR proteins. The consensus for the N-terminal Cys-rich cluster is also shown. The chromosomal arrangement of the various SLRP genes is shown in a telomeric orientation (right). Transcriptional direction is shown by the arrows above the color-coded boxes. The horizontal distance between genes is not to scale. This figure was modified after Henry et al.

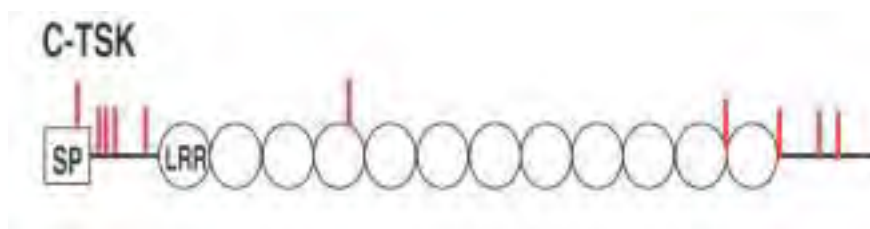


Figure 2'. Schematic drawing of the primary structure of C-TSK. LRRs are indicated as circles. Cysteine residues are indicated as red bars. SP, signal peptide. (Ohta et al., 2004)

1-2. Background and Specific Aims

Background

We previously described the isolation of Tsukushi (TSK) isoforms (Ohta et al., 2004; Ohta et al., 2006), soluble molecules belonging to the Small Leucine-Rich Proteoglycan (SLRP) family (Iozzo, 1997; Hocking et al., 1998; Schaefer and Iozzo, 2008), and showed that TSK works as extra-cellular modulators of pivotal signaling cascades acting during early embryonic development in chick and frog (Ohta et al., 2004; Ohta et al., 2006; Kuriyama et al., 2006; Morris et al., 2007). Originally, TSK was identified using signal sequence trap screening from chick lens library. In the pilot study, we found that TSK was strongly expressed in the ciliary body (CB), where retinal stem/progenitor cells located. Furthermore, TSK was also expressed subventricular zone (SVZ) and subgranular zone (SGZ), where brain stem cells exist.

Although the mammalian central nervous system (CNS) was previously thought to be incapable of regeneration, this possibility has been reassessed after the identification of neural stem/progenitor cells localized in specific compartments of the adult CNS. Multipotent stem/progenitor cells have also been isolated from the CB at the anterior margin of the adult mouse and human retina (Ahmad et al., 2000; Tropepe et al., 2000; Coles et al., 2004), and they have been shown in vitro to possess several universal characteristics of stem cells, including proliferation, clonogenicity, self-renewal, and multi-potent differentiation capacity (Ahmad et al., 2000; Tropepe et al., 2000; Inoue et al., 2006). Several lines of evidence suggest that Wnt signaling promotes proliferation of neural stem cells, while restraining their differentiation during development (Chenn and Walsh, 2002, 2003; Inoue et al., 2006; Ito et al., 2007; Kalani et al., 2008; Kubo et al., 2005; Reya et al., 2003). Nonetheless, little is known about the molecular

mechanisms that control stem cell self-renewal and neurogenesis and restrict tissue-specific stem cells to specific compartments or niches such as the retinal CB and the SVZ remain largely unclear.

Specific Aims

- a) I analyzed whether TSK regulates Wnt signaling and controls the retinal stem/progenitor cells proliferation as a niche molecule.
- b) I examined whether TSK is also involved in regulation for stem/progenitor cells proliferation and differentiation in the brain.
- c) I examined the anterior commissure formation in the TSK^{-/-} mouse brain

2. Materials and Methods

2.1 chick embryos

Fertilized chick eggs were purchased from a local farm (Takeuchi, Japan) and incubated at 38°C in a humidified chamber until they reached the appropriate embryonic stages (Hamburger and Hamilton, 1951).

2.2 In situ hybridization

Sense and antisense riboprobes labeled with digoxigenin (DIG) were synthesized from a pBluescript construct (SK-) containing 800-bp fragment of Chick-TSK, Chick-Wnt2b (C-Wnt2b), Chick-Frizzled4 (C-Frz4), Chick-Frizzled5 (C-Fzd5), Chick-BMP7 cDNA using T7 and T3 RNA polymerases, respectively.

Chick embryo eyes were fixed in 4% paraformaldehyde in PBS at room temperature (RT) for 1h. For section in situ hybridization, fixed embryos were cryoprotected by immersion in 20% sucrose in PBS at 4°C overnight and embedded in OTC compound (Sakura Fine Technical Co. Ltd, Tokyo, Japan). Sections were collected 12 µm thickness on mas-coated slide glasses (Matunami, Japan). In situ hybridization was performed using the method of Schaeren-wiemers and Gerfin-Moser (1993). Sections were incubated in 1µg/ml proteinase K solution for 5min at RT and permeabilized with 1% Triton X-100 for 30 min, and then pre-hybridized with herring sperm 10mg/ml DNA for 2h at 65°C. Hybridization was performed overnight at 55°C with 0.1ng/ml probe in hybridized solution. After hybridization, sections were washed in 50% formamide/2XSSC at the hybridization temperature and block with 5mg/ml blocking reagent (Rosh). The mRNA expression was visualized using an alkaline phosphatase

(AP)-conjugated anti-DIG Fab fragment (Rosh) 1:2500 dilution in blocking reagent solution. Cooler reaction employed 337.5µg/ml p-nitroblue tetrazolium(NBT) and 175µg/ml 5-bro,o-4chloro-3-indolylphosphate(BCIP) in NTMT solution [0.1M Tris-HCl (pH9/5), 0.1M NaCl, 50mM MgCl₂] 6-72h at 4 °C in the dark. Slides were dried overnight, dehydrated in ethanol and xylene, and then mounted.

2.3 In ovo electroporation

Electroporated embryos were incubated approximately 48h HH stage10. I made a small window on top of the egg and place one drop of 1xTyrode on the embryos. To visualize the embryo black ink/1×tyrode was injected under the embryo. Using glass capillaries, RCAS plasmid DNA/Fast green was injected into the optic vesicle. The concentration of DNA is 5µg/µl. Electric square pulses were 7V, two times length of 30 ms and pulse intervals 50 ms. After the electoporation, the window was sealed with clear tape and incubated 37.5°C for 7days. Embryo was harvested and fixed 4% PFA/PBS for 1h at RT and cryopreserved in 20% sucrose in PBS at 4°C overnight.

2.4 Mice

Tsukushi null mutant mice were generated by inserting a LacZ/Neo cassette into the TSK coding exon (Figure 1). The mice used in these studies were backcrossed to the C57BL/6J strain for at least six generations and can be considered of an almost uniform genetic background. All experiments on mice were conducted in accordance with the guidelines of the Kumamoto University Center for Animal Resources and Development.

2.5 Tissue processing

Deeply anesthetized mice were transcardially perfused with 25 ml phosphate-buffered saline (PBS) and fixed with 4% paraformaldehyde in PBS. Mouse brains were harvested and post-fixed in the same fixative at 4°C overnight. Brains were sliced into sections of 50-100 µm thickness using a Vibratome 2000 (Leica) for immunostaining.

2.6 Immunohistochemistry

To inactivate the endogenous peroxidase activity, the sections were treated with a solution of 3% H₂O₂/0.3% Triton-X in PBS (PBST) for 15 min at room temperature (RT). Sections were incubated with 10% normal donkey serum in PBST to block nonspecific binding for 1 hr at RT and incubated with each of the primary antibodies at 4 °C overnight, washed with 0.3% PBST (3 x 10 min), and incubated with secondary antibodies for 2 h at RT. After being washed with PBST (3 x 10 min), the sections were subsequently incubated with an avidin-biotin-peroxidase complex (ABC Kit Standard, Vector Laboratories) for 1 h at RT. The antibody-peroxidase complex was visualized using a VIP peroxidase substrate kit (Vector Laboratories).

2.7 Hematoxylin and Kluver-Barrera (KB) staining

For the axonal morphological analysis, adult brain sections were stained with hematoxylin/eosin (HE) using standard methods. For double staining with hematoxylin and Kluver-Barrera (KB), the sections were incubated with 0.1% Luxol fast blue at 56 °C overnight and washed in 95% ethanol for 5 min at RT. After being washed with PBS, the sections were differentiated briefly in a 0.05% lithium carbonate solution, rinsed twice with 70% ethanol, and washed with PBS. After hematoxylin staining, the sections were dried at RT and cleared with xylene.

2.8 Antibodies

The following antibodies were used for immunohistochemistry: rat anti-L1, 1:5000 (Chemicon); goat anti- β -gal, 1:500 (CAPEL); rabbit anti- β -gal, 1:10000 (CAPEL); mouse anti-neurofilament (2H3) (Hybridoma Bank), biotin-labeled anti-rat IgG, 1:500 (Southern Biotechnology Associates); FITC-conjugated anti-rat IgG, 1:500 (Jackson); and Cy3-conjugated anti-rabbit IgG, 1:500 (Jackson).

2.9 DiI labeling

To trace the AC axonal tract, a 5% solution of 1,1'-dioctadecyl-3,3,3',3'-tetramethylindocarbocyanine perchlorate (DiI) (Molecular Probes) was injected into the AON region on days P2 and P5, and the brains were analyzed on days P3 and P7, respectively. Animals were transcardially perfused with PBS and fixative, and horizontal sections of the brains (100 μ m thickness) were cut on a vibratome.

3. Results

3-1: Part A

Tskushi functions as a Wnt signaling inhibitor by binding to Frizzled4 in competition with Wnt2b

3-1-1: TSK expression in the adult mouse eye

In order to address TSK function in vivo, we established TSK^{-/-} mice by inserting a lacZ/Neo cassette into the TSK coding exon (Figure 1 A; Murata et al., 2004; Yagi et al., 1993). TSK^{-/-} mice are viable and fertile. We then examined the expression domain of TSK in the adult eye by β -gal staining of adult TSK^{+/-} eyes (8-10 weeks old). We found β -gal activity in retinal layers, the CB, and the lens epithelium (Figures 2A and B). This expression pattern is also conserved in frog and chick (data not shown). In the differentiated retina, some cells in the inner nuclear layer and a few cells in RGC later express TSK although the expression is much weaker than those in the CB (Figure 2C). The expression pattern of TSK in the CB was further examined by immunostaining with anti-pax6 and anti- β -gal antibodies (Figures 2E-I). As shown in Figure 2D, the CB is composed of folds of bi-layered epithelium, with an outer non-pigmented layer, and an inner pigmented layer. Inside of these epithelial folds, the inner surface of the pigmented layer forms a complex tri-dimensional network with capillaries (Morrison et al., 1996). Pax6 expression was detected in most of the cells of the CB epithelium, encompassing both the pigmented and non-pigmented layers (Lord-Grignon et al., 2006), whereas TSK was predominantly expressed in the outer non-pigmented layer (Figures 2H and I).

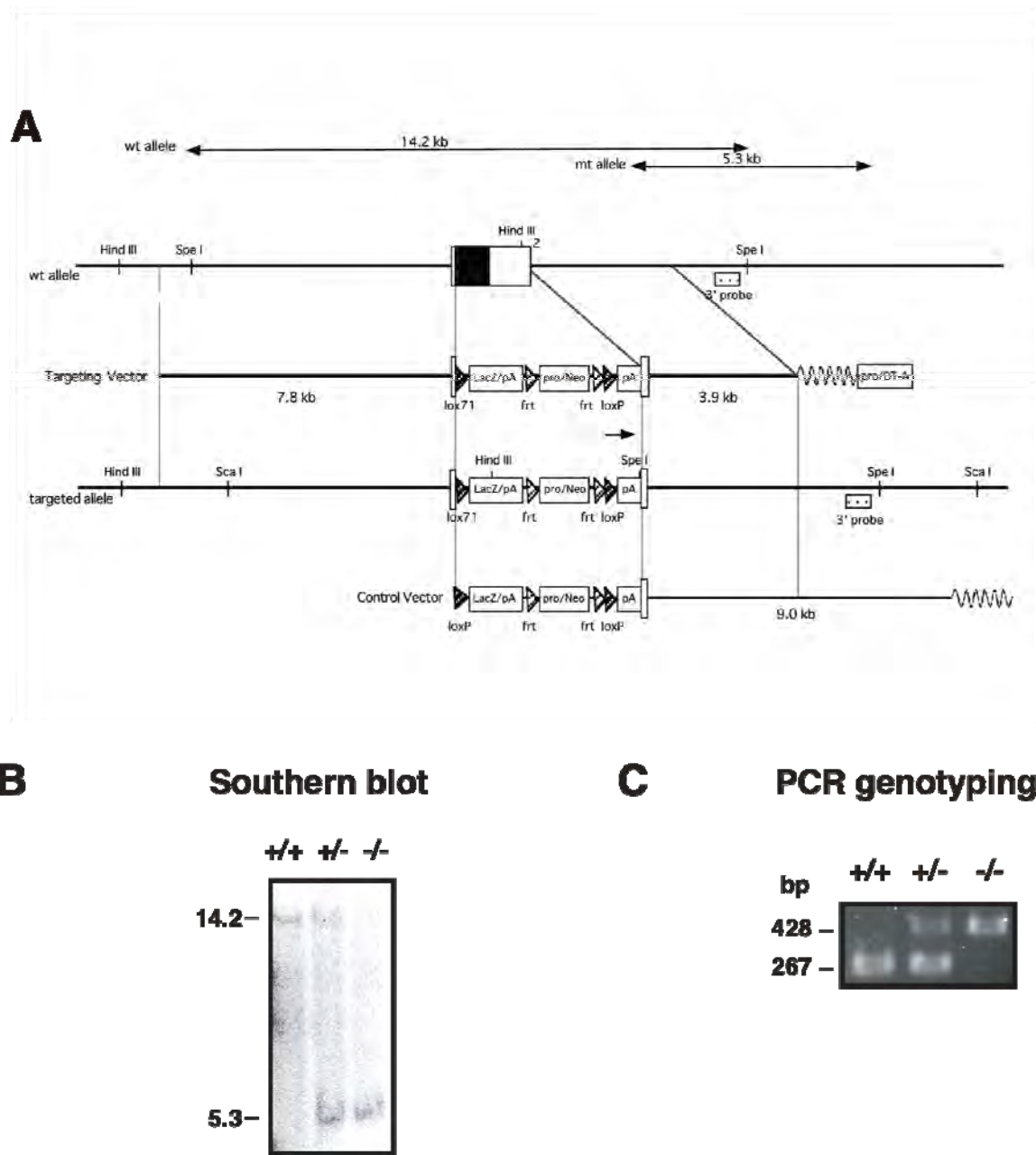


Figure 1. Mutant Mouse. (A and B) A targeting vector for TSK was constructed, and the Tsukushi mutant mice (Acc. No. CDB0547K) were generated as described^{24,25}. (C) PCR amplification for genotyping was performed on templates of unpurified tail lysates with the following set of primers: 5'-cccagcagtagcaacaacaa-3' (TSK-S), 5'-gagcttgtaagtccttgga-3' (TSK-AS), and 5'-gatcccatcaagcttatcg-3' (LacZ). TSK-S and TSK-AS amplified a 267 bp fragment identifying the wild-type allele, while lacZ and TSK-AS amplified a 428 bp fragment, corresponding to the null allele.

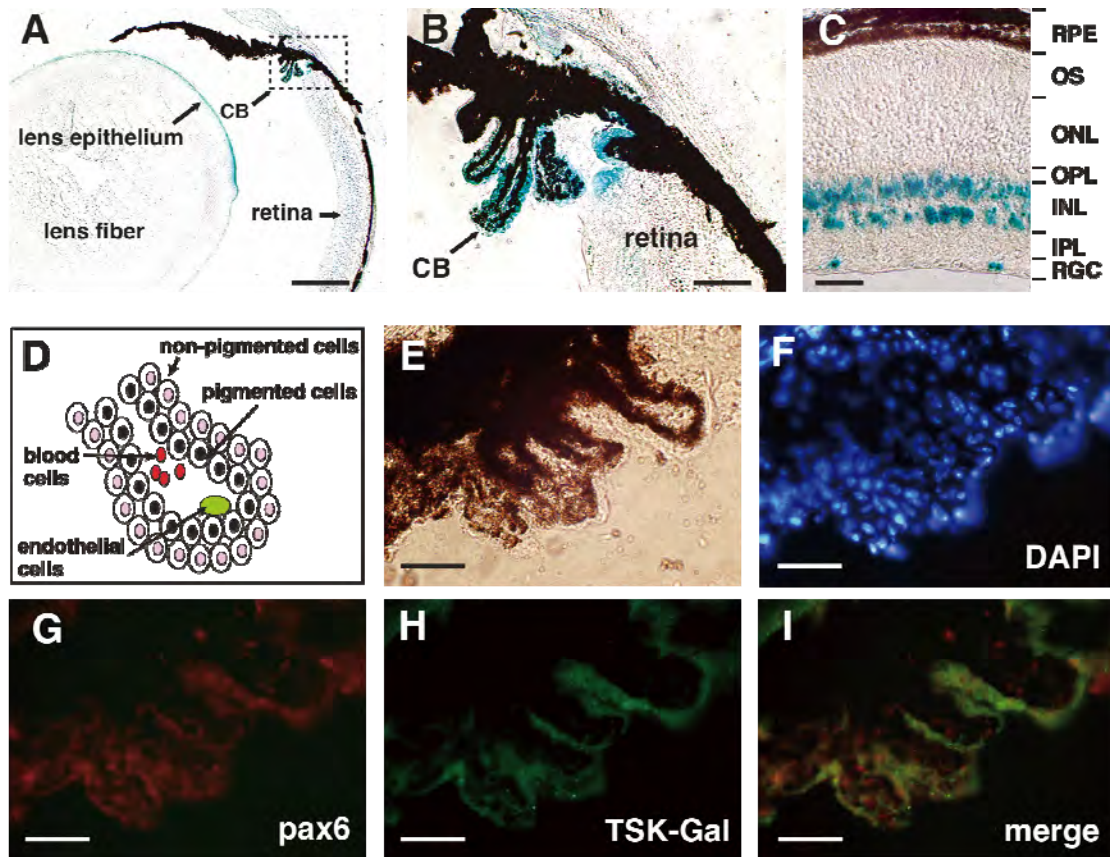
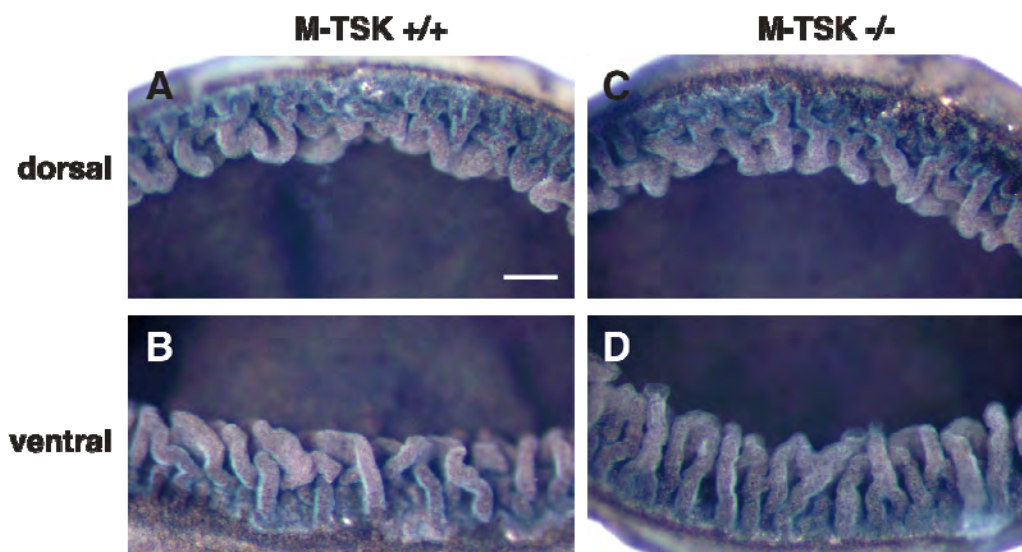


Figure 2. Expression of TSK in Adult Mice Eye. (A) Detection of β -gal activity in the adult eye of TSK $^{+/-}$ mice. TSK is strongly expressed in the lens epithelium and CB. (B) Magnified view of the area framed in (A). (C) Expression of TSK in the INL and RGC of TSK $^{+/-}$ mice. Scale bar, 350 μ m in (A); 100 μ m in (B); 40 μ m in (C). (D) Schematic drawing of the cellular organization of the CB. (E) Bright field image of the CB from one adult eye of a TSK $^{+/-}$ mice. (F) Nuclear staining of (E) with DAPI. (G) Immunostaining of (E) with anti-pax6 antibody. (H) Immunostaining of (E) with anti-b-gal antibody. (I) Merged image of (G) and (H). CB, ciliary body; RGC, retinal ganglion cell layer; IPL, inner plexiform layer; INL, inner nuclear layer; OPL, outer plexiform layer; ONL, outer nuclear layer; OS, outer segments; RPE, retinal pigmented epithelium. Scale bars = 50 μ m in I, G and H.

3-1-2: Loss of TSK results in expansion of CB in vivo

To elucidate the role of TSK in the CB of the retina, we performed the morphological analysis of adult eyes from TSK^{-/-} and wild type (WT) by observing the CB structure from the vitreous side. Figures 3A and 3B respectively show the CB structure in the dorsal and the ventral regions of a WT eye. We noticed that the ventral CB (Figure 3B) is larger than the dorsal CB (Figure 3A). Both the ventral and the dorsal CB appeared to be expanded in TSK^{-/-} eyes compared to WT eyes, although a dorso-ventral difference was maintained in mutant eyes (Figures 3C and D). This effect was quantified by measuring the maximal CB length in the dorsal and ventral regions of TSK^{-/-} (n=12) and WT eyes (n=10) (Figures 3E and F). Histological analysis confirmed the expansion of the CB in TSK^{-/-} eyes (n=10) (Figures 3G and I) compared to WT eyes (n=8) (Figures 3H and J), as detected by measurements of CB area on serial sections of TSK^{-/-} and WT eyes (Figure 3K).



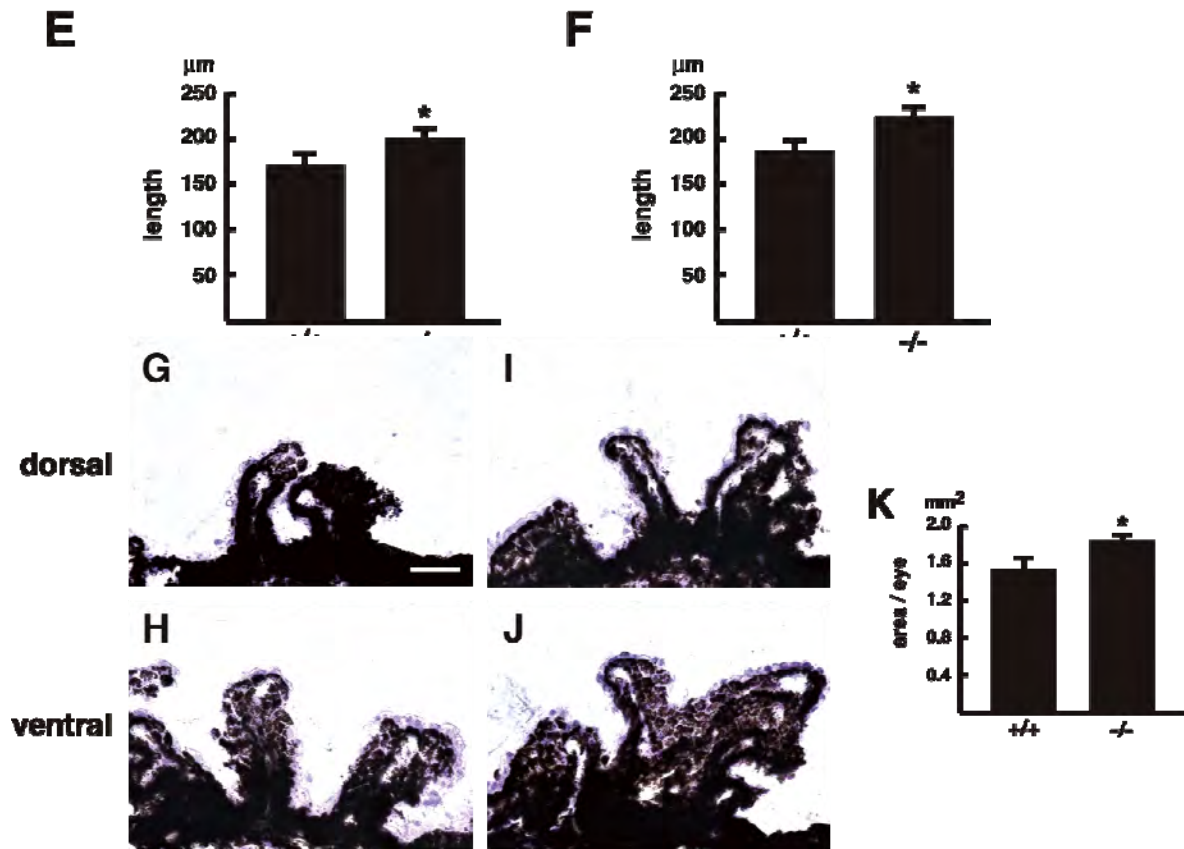
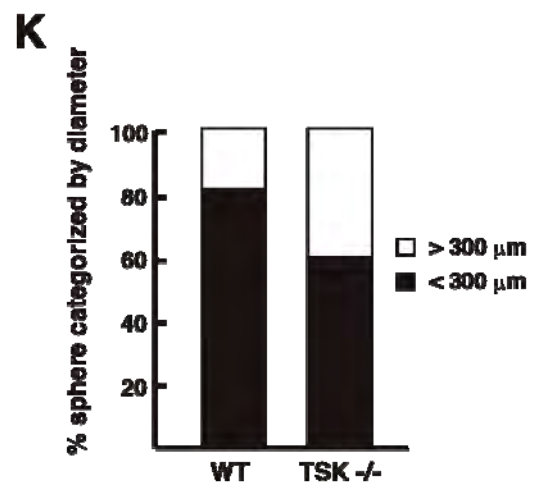
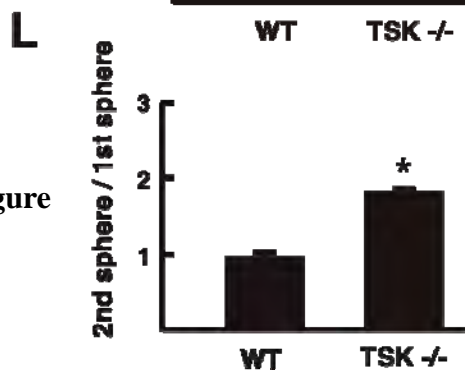
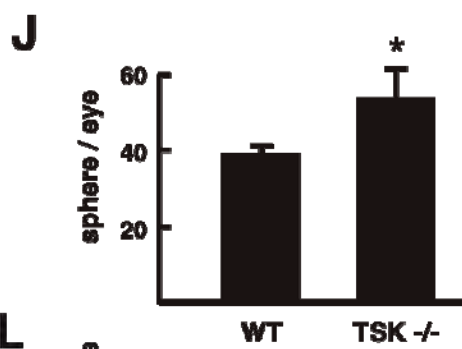
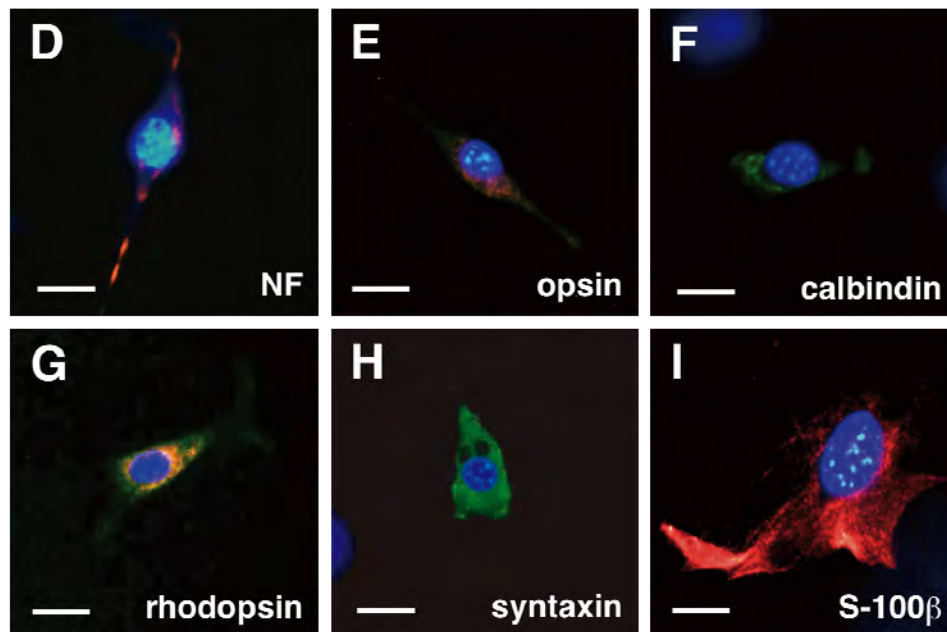


Figure 3. Expansion of CB in TSK^{-/-} Mice Eye. (A-D) The CB structure of dorsal (A, C) and ventral (B, D) areas of the adult TSK^{-/-} (C, D) and TSK^{+/+} mice eye (A, B). Scale bars, 100 μm. (E and F) Quantification of the length of the CB in TSK^{+/+} and TSK^{-/-} mice. (E) Dorsal area. (F) Ventral area. Asterisk, $p < 0.001$ based on a two-tailed Student's *t*-test. (G-J) Hematoxylin-stained sections of the CB area from representative eyes of TSK^{-/-} (I, J) mice as compared to TSK^{+/+} (G, H) mice. (K) Quantification of the size of the CB area in TSK^{+/+} and TSK^{-/-} mice. Asterisk, $p < 0.001$ based on a two-tailed Student's *t*-test. Error bars represent the SD. Scale bars = 40 μm in G.

3-1-3: Effects of TSK on retinal spheres in vitro

To gain more insight into the function of TSK in the adult eye, we isolated and compared the behavior of retinal spheres generated from adult WT and TSK^{-/-} CB (Figure 4A). As shown in Figure 4B, TSK expression was detectable by RT-PCR in retinal spheres from WT but not TSK^{-/-} mice. We also detected expression of mouse Wnt2b (homologous to chick Wnt2b) and Fzd4 in retinal spheres (Figure 4C). When retinal spheres from the adult WT or TSK^{-/-} mice were triturated and cultured under conditions that promote retinal cell differentiation (Ahmad et al., 2000; Inoue et al., 2006; Tropepe et al., 2000), both WT and TSK^{-/-} cells were similarly capable of differentiating along neuronal- and glial-pathways, indicating that TSK is not required for retinal cell differentiation (Figures 4 D-I). However, comparison of the number of retinal spheres isolated from WT and TSK^{-/-} mice (Figure 4J) showed that the number of spheres from TSK^{-/-} mice (54 ± 7.9 , $n=24$) was significantly higher than those from WT mice (38 ± 1.4 , $n=24$). We also measured the diameter of individual retinal spheres. The percentage of retinal spheres whose diameter was greater than 100 μm was 18.5% (200 ± 93 μm , $n=492$) in the case of WT mice, while it was increased to 40.8% (283 ± 122 μm , $n=472$) in TSK^{-/-} spheres (Figure 4K). We then dissociated WT or TSK^{-/-} retinal spheres into single cells, and allowed them to form secondary spheres in the presence of FGF2 (Ahmad et al., 2000; Tropepe et al., 2000). The number of secondary sphere colonies from TSK^{-/-} primary spheres was greater than the number generated from WT spheres (Figure 4L). Altogether, in vivo and in vitro analysis of the CB of WT or TSK^{-/-} eyes or of the retinal spheres derived from them indicate that TSK function is required for proper CB size, possibly by regulating proliferation of the stem/progenitor cells located in it (Ahmad et al., 2000; Tropepe et al., 2000).



Figure

4. TSK Inhibits Proliferation of Retinal Spheres. (A) A wild type retinal sphere after 7 days culture. Scale bar, 100 μm . (B) RT-PCR showing the expression of TSK in spheres derived from wild type but not TSK^{-/-} mice. (C) Expression of Wnt2b, and Fzd4 in wild type retinal spheres as detected by RT-PCR. Sphere cells from adult TSK^{-/-} mice were triturated and cultured under condition that promote retinal cell differentiation for 7 days. We were able to demonstrate the presence of markers for different differentiated retinal cells. (D) NF (neurofilament) (retinal ganglion cells and bipolar cells), (E) opsin (cone photoreceptor cells), (F) calbindin (horizontal cells and amacrine cells), (G) rhodopsin (rod photoreceptor cells), (H) syntaxin (amacrine cells), (I) S-100b (Müller glia). (J) Quantification of the number of spheres generated from the CB of adult wild type or TSK^{-/-} mice. Asterisk, $p < 0.05$ based on a two-tailed Student's *t*-test. (K) Quantification of the percentages of wild type or TSK^{-/-} spheres with a diameter smaller or bigger than 100 μm . (L) Quantification of the Number of secondary spheres generated from wild type or TSK^{-/-} primary spheres. Asterisk, $p < 0.001$ based on a two-tailed Student's *t*-test. Error bars represent the SD. Scale bars = 20 μm in D-I.

3-1-4: Expression of TSK at the peripheral chick retina.

There is substantial evidence that the Wnt signaling pathway controls development of peripheral eye structures in several animal model. TSK is expressed in the peripheral region of the developing chick eye at E6 (Figures 5A and B). As shown in Figure 1C, Wnt2b expression is localized to the anterior-most tip of the optic cup, whereas chick TSKB (C-TSKB) (Ohta K et al., 2006) is expressed in the adjacent iris epithelium (Figure 5B). Comparison with the expression pattern of Collagen IX (Figure 5F), a marker of the neighboring ciliary epithelium (Cho & Cepko, 2006; Dhawan & Beebe, 1994) showed that C-TSKB expression does not extend into this region. Fzd4 are expressed in both the ciliary and iris epithelia, whereas Fzd5 expression was not detectable in these areas (Figures 5D and E). These expression patterns suggest that Wnt2b and C-TSKB could functionally interact with each other and regulate Fzd-dependent signaling in the peripheral eye.

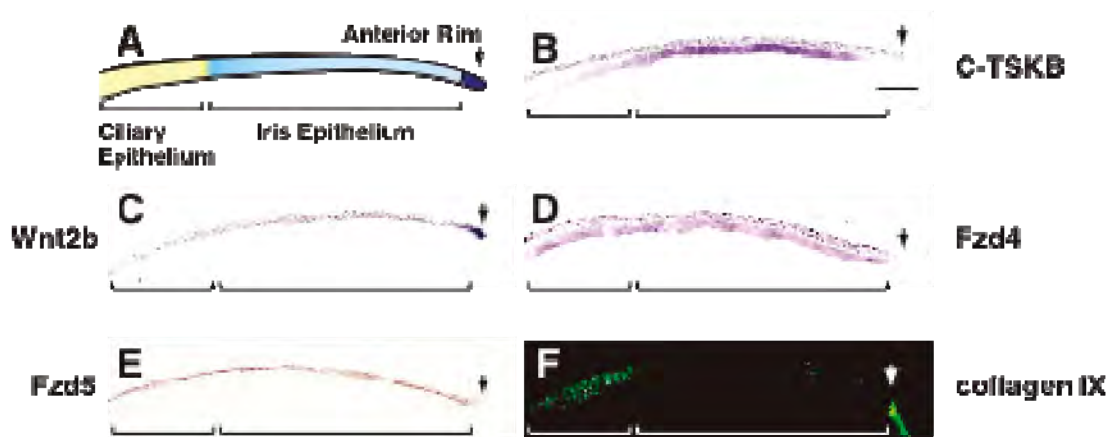


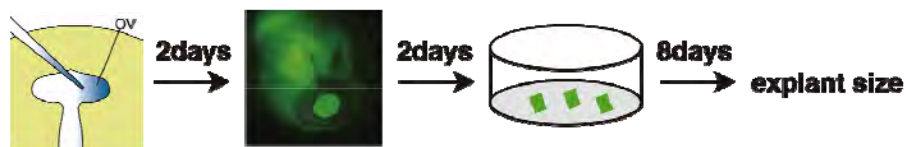
Figure 5. Expression of TSK at the Peripheral Chick Retina. (A) Schematic drawing of the peripheral region of chick eye at E6. (B-E) mRNA expression of C-TSKB (B), Wnt2b (C), Fzd4 (D), and Fzd5 (E) in the peripheral areas of E6 chick retinas. (F) Collagen IX protein expression in the ciliary epithelium. Arrowheads in (A-F) point to the anterior rim of the retina. Scale bars = 100 μm in B.

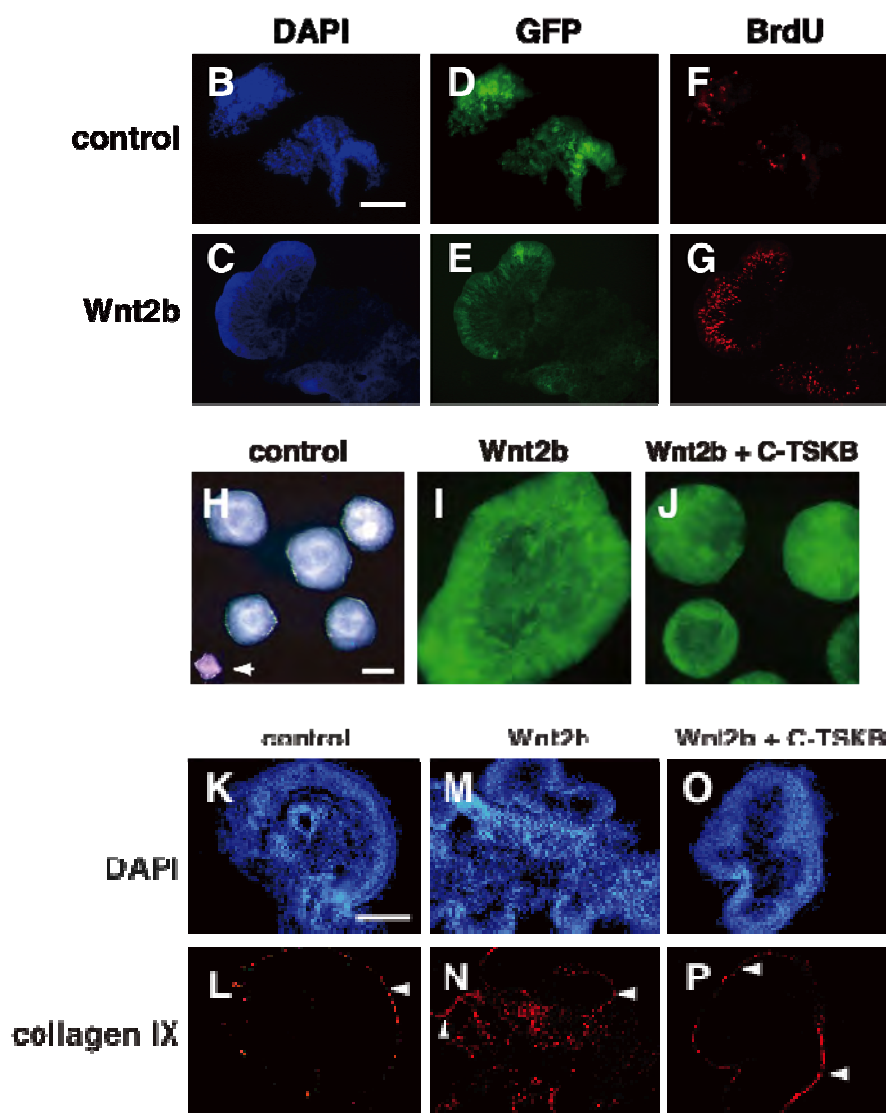
3-1-5: TSK inhibits Wnt2b activity in vitro.

In order to address whether TSK functions as a Wnt inhibitor, we co-overexpressed C-TSKB with Wnt2b into the chick optic vesicle and observed their effects on the proliferation of retinal explants, which is known to be stimulated by Wnt2b (Kubo et al., 2005). We first electroporated optic vesicles of E1.5 chick embryos with a Wnt2b-expressing provirus as previously described (Kubo et al., 2005). Explants of electroporated retinal tissues (250 x 250 mm² surface area) were then dissected from the central region of E5.5 retinas and cultured in vitro for 8 days (Figure 6A). Confirming the results of previous studies (Kubo et al., 2005), Wnt2b-expressing retinal explants generated large folded sheets of tissue (Figure 6I). Moreover, a number of cells incorporated 5-bromo-2-deoxyuridine (BrdU) in Wnt2b-expressing explants (Figures 6B-G), whereas co-expression of RCAS: Wnt2b with RCAS: C-TSKB resulted in explants of similar size to that of control explants (Figures 6H and J). As a positive control for Wnt2b activity in this assay, we also employed the ability of Wnt2b to induce ectopic Collagen IX expression in retinal explants (Figures 6M and N) and this ectopic induction was prevented in explants co-expressing Wnt2b and C-TSKB (Figures 6O and P), which lacked Collagen IX expression similar to control explants (Figures 6K and L) (26). Furthermore, we dissociated electroporated explants into single cells and quantified the number of cells (Figure 6Q). The cell number of Wnt2b and C-TSKB co-expressing explants ($7.2 \pm 0.4 \times 10^3$, n=30) was similar to that of control explants ($4.3 \pm 1.3 \times 10^3$, n=30) and C-TSKB expressing explants ($4.6 \pm 1.7 \times 10^3$, n=30); however, that of Wnt2b expressing explants was exponentially increased ($1.2 \pm 0.1 \times 10^5$, n=30) (Figure 6Q). These results were not due to the cell death in the explants during the culture (data not shown). We next sought to identify specific subdomains of TSK involved in the inhibition for Wnt activity. For this purpose, we generated Fc-fusion

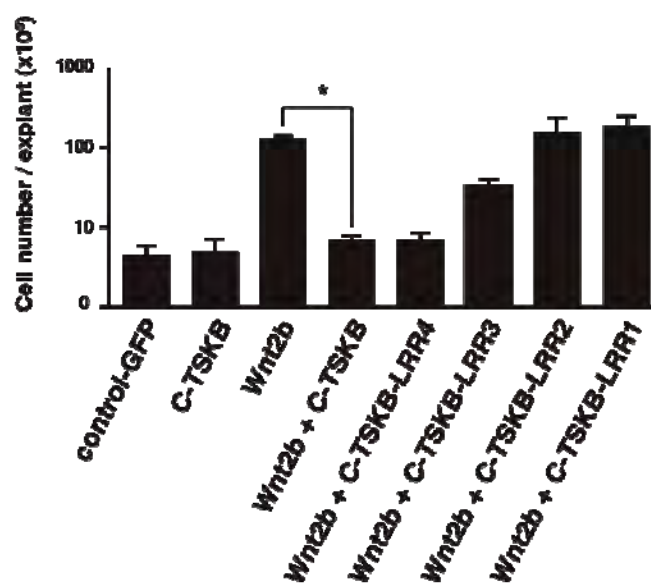
constructs encoding four LRR domains (CTSKB-LRR4-Fc), three LRR domains (CTSKB-LRR3-Fc), two LRR domains (CTSKB-LRR2-Fc), or a single LRR domain (CTSKB-LRR1-Fc) from the N-terminal and evaluated their inhibitory function on Wnt2b activity using similar electroporation assays. Only CTSKB-LRR4-Fc was able to completely inhibit Wnt activity in vitro (CTSKB-LRR4-Fc; $7.3 \pm 0.6 \times 10^3$, n=22; CTSKB-LRR3-Fc; $3.0 \pm 0.7 \times 10^4$, n=32; CTSKB-LRR2-Fc: $1.4 \pm 0.6 \times 10^5$, n=20; CTSKB-LRR1-Fc: $1.7 \pm 0.4 \times 10^5$, n=20) (Figure 6Q). Thus, at least four LRR domains of the CTSKB protein appear to be necessary for robust Wnt signaling inhibition. To examine the specificity of the inhibition of Wnt2b activity by C-TSKB, we co-electroporated embryos with Wnt2b together with either the extracellular domain of LINGO-1 (Okafuji & Tanaka, 2005), containing 12 leucine-rich repeat domains (LINGO-1-ex), or the secreted proteins Akhirin (Ahsan et al., 2005) or Equarin (Mu et al., 2003), which are not related to the SLRP family. None of these proteins inhibited Wnt activity (Figure 6R).

A





Q



R

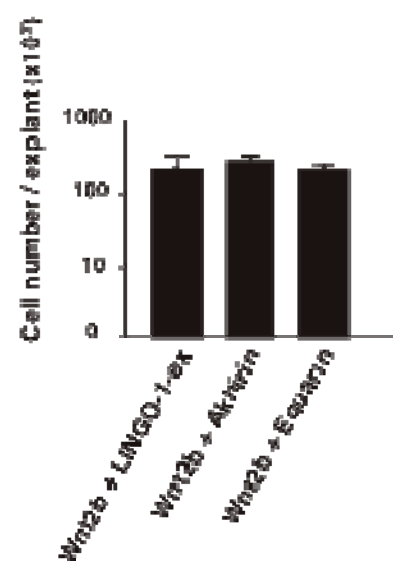
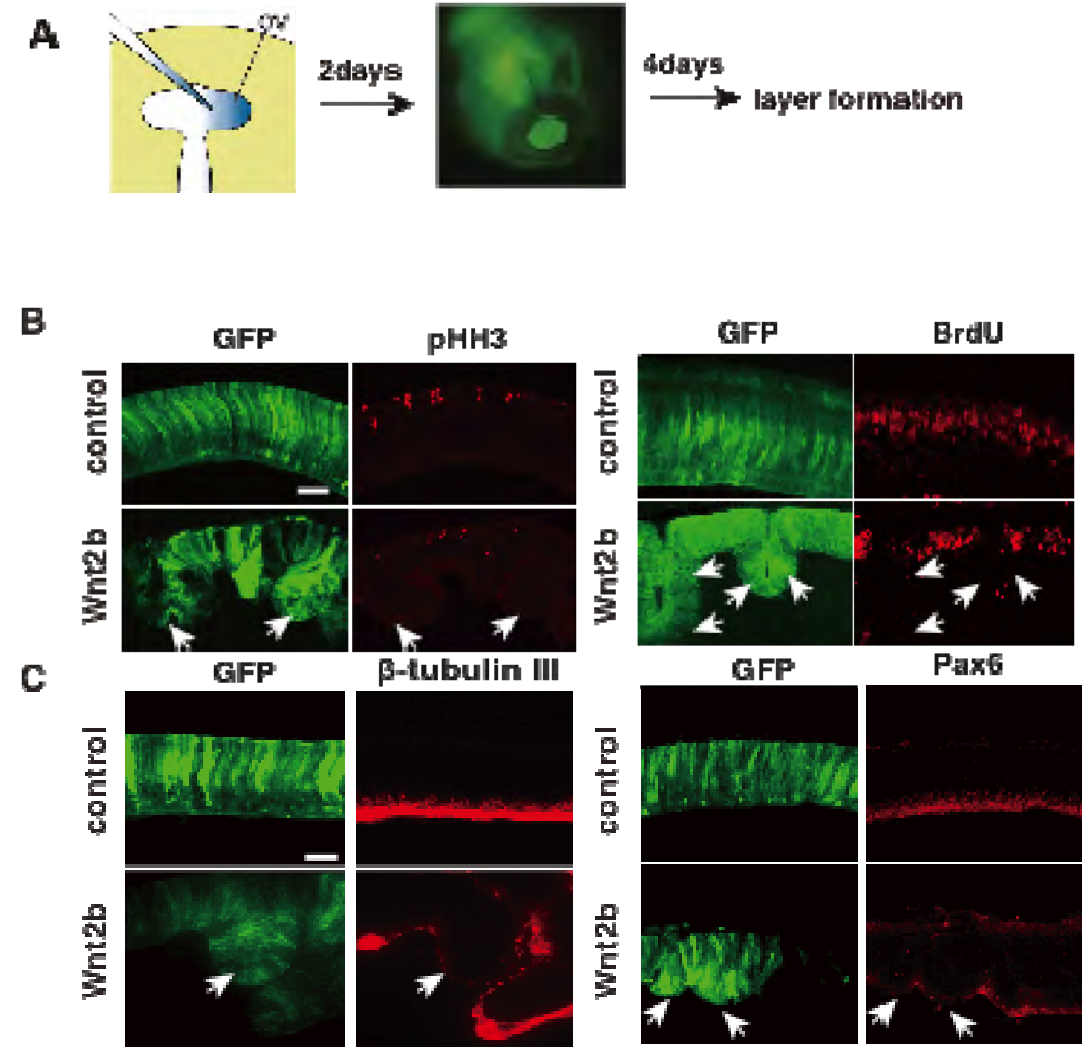


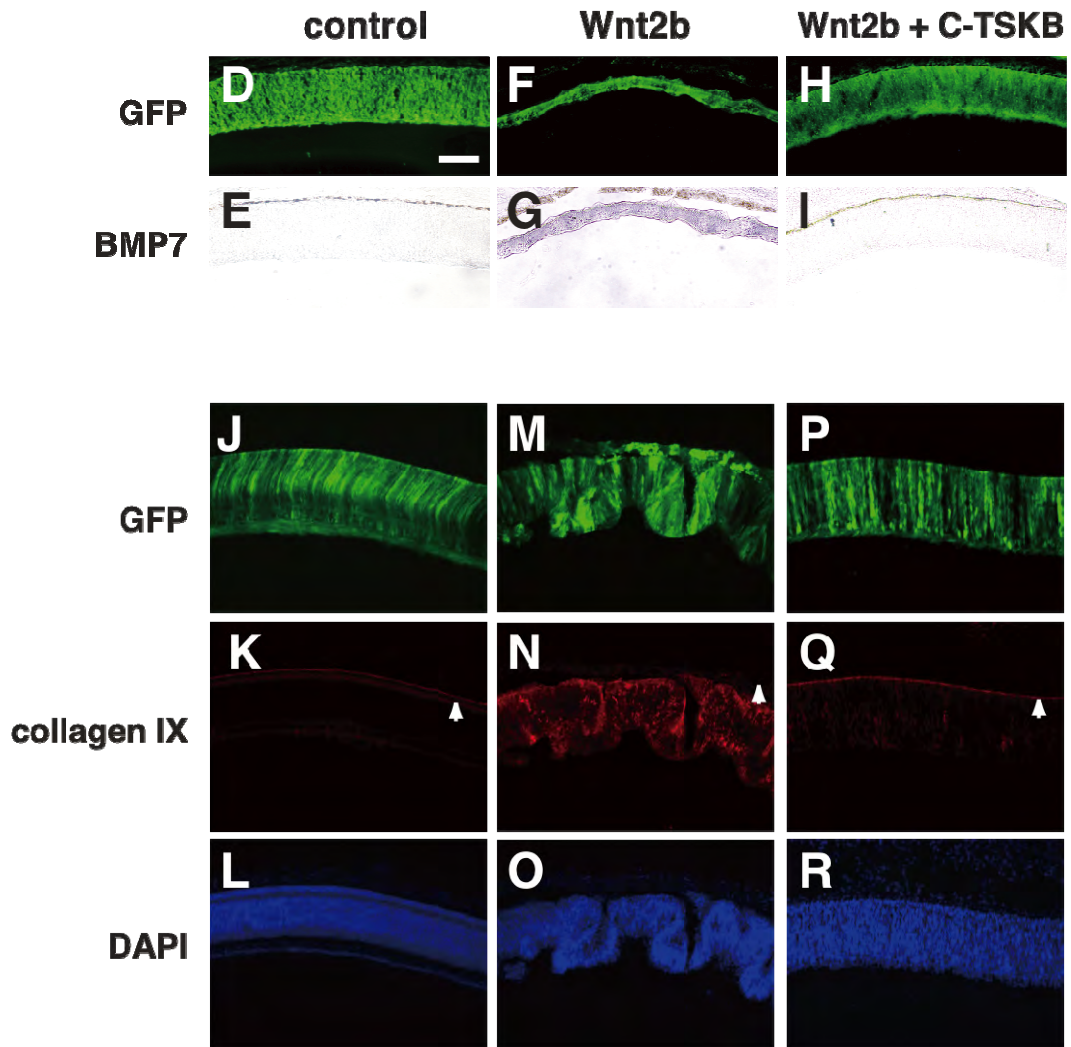
Figure 6. TSK Inhibits Wnt Activity In Vitro. (A) Schematic drawing of the experimental procedure. (B-G) BrdU incorporation was increased in the explants expressing Wnt2b. (B, C) DAPI, (D, E) GFP, (F, G) BrdU. Scale bar, 100 μ m. (H-J) Retinal explants of control (H), Wnt2b- (I), Wnt2b+C-TSKB-expressing chick retinas (J), which were dissected out at E5.5 chick and cultured for 8 days in vitro following electroporation at E1.5. The arrow in (H) points to an explant immediately after dissection. RCAS-EGFP was co-transfected to visualize electroporated cells. (K-P) Expression of Collagen IX in the explants expressing Wnt2b. (K, M, O) DAPI, (L, N, P) Collagen IX. White arrowheads indicate the immunoreactivity of anti-Collagen IX antibody on the choroid. (Q) Quantification of cell numbers in explants electroporated with the indicated DNA constructs. Note that at least four LRR domains are necessary and sufficient to inhibit the effects of Wnt2b on cell proliferation in vitro. Asterisk, $p < 0.001$ based on a two-tailed Student's t-test. Error bars represent the SD. (R) For the in vitro assay, we co-electroporated embryos with Wnt2b together with either the extracellular domain of LINGO-1 containing 12 leucine-rich repeat domains (LINGO-1-ex), or the secreted proteins Akhirin or Equarin, which are not related to the SLRP family. None of them inhibited Wnt activity (LINGO-1-ex; $2.5 \pm 0.8 \times 10^5$, $n=40$; Akhirin; $2.8 \pm 0.2 \times 10^5$, $n=40$; Equarin; $2.0 \pm 0.3 \times 10^5$, $n=30$). Scale bars = 180 μ m in B, H and K.

3-1-6: TSK inhibits Wnt2b activity in vivo.

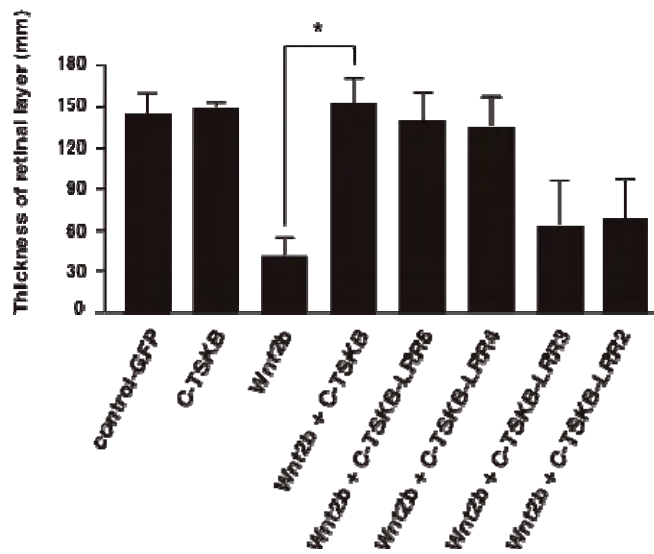
Overexpression of constitutively active β -catenin or Wnt2b in the optic vesicle in vivo was previously shown to induce specification of peripheral structures, namely the ciliary epithelium and the iris epithelium, and decrease retinal cell proliferation (Cho & Cepko, 2006). We used this assay in order to examine whether the inhibitory activity of C-TSKB on Wnt signaling can also be observed in vivo (Figure 7A). RCAS:Wnt2b was infected into the developing optic vesicle at E1.5 and infected eyes were examined at E7.5. Confirming previous studies, we also observed specification of peripheral cell fates and a significant reduction in the number of proliferating cells in Wnt2b infected regions (Figure 7B) and downregulation of β -tubulin III and pax6 expression (Figure 7C). The infected eyes showed thinning and folding of the retinal epithelium at the level of the central retina, upregulation of the peripheral markers BMP7 and Collagen IX (Figures 7F, G, M-O) (Cho & Cepko, 2006; Dhawan & Beebe, 1994). The average thickness of the RCAS-Wnt2b-infected thinner retina was $40 \pm 19 \mu\text{m}$ ($n=11$) (Figure 7S). In the presence of both Wnt2b and C-TSKB, the infected retinal tissue failed to show any abnormalities (Figures 7H, I, P-R) and was similar to the control retina (Figures 7D, E, J-L). The average thickness of control-, RCAS: CTSKB- and RCAS: Wnt2b+RCAS: C-TSKB-infected retina was $142 \pm 21 \mu\text{m}$ ($n=8$), $147 \pm 6 \mu\text{m}$ ($n=3$), and $151 \pm 26 \mu\text{m}$ ($n=7$), respectively (Figure 7S). Then, we performed the same experiments using mutant forms of C-TSK used in Figure 2. The average thickness of CTSKB-LRR2-Fc, CTSKB-LRR3-Fc, CTSKB-LRR4-Fc, or CTSKB-LRR6-Fc-infected retina was $72 \pm 28 \mu\text{m}$ ($n=4$), $65 \pm 33 \mu\text{m}$ ($n=4$), $132 \pm 23 \mu\text{m}$ ($n=4$), and $143 \pm 22 \mu\text{m}$ ($n=4$), respectively (Figure 7S). Thus, similar to the in vitro assay shown in Figure 6, at least four LRR domains are necessary and sufficient to

inhibit the effects of Wnt2b in vivo (Figure 7S). In this same assay, infection of RCAS:Wnt2b with RCAS:LINGO-1-ex, RCAS:Akhirin, or RCAS:Equarlin failed to inhibit Wnt2b activity (Figure 7T). Taken together, these results indicate that TSK specifically and efficiently abrogates Wnt2b activity both in vivo and in vitro.





S



T

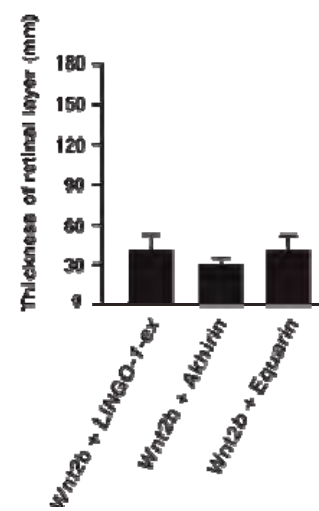
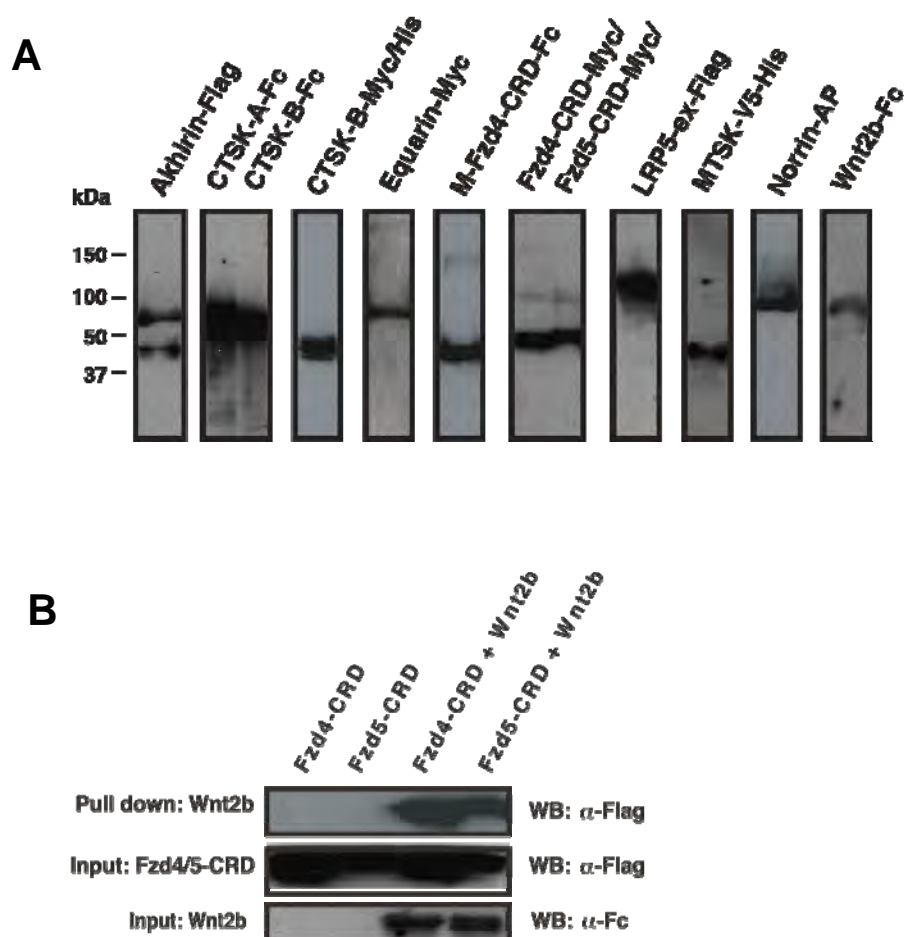


Figure 7. TSK Inhibits Wnt Activity In Vivo. (A) Schematic drawing of the experimental procedure. Assay for retinal progenitor proliferation in vivo. (B and C) Representative images of an RCAS-GFP or RCAS:Wnt2b-infected retina at E7.5 showing pH3 and BrdU incorporation in the central retina. For in vivo labeling, 0.3 ml of 6 mg/ml BrdU was injected to the yolk 30 min prior to harvesting. Note that, in the Wnt2b expressing retina, a significant reduction in the number of pH3- and BrdU-labeled cells was observed in extensively infected regions (arrows). (C) Effects of Wnt2b on retinal cell differentiation. Immunohistochemistry for β -tubulin III (a marker of ganglion and amacrine cells) and pax6 (a marker for horizontal and amacrine cells) in RCAS-GFP and RCAS-Wnt2b infected retinas. Note that, in the Wnt2b expressing retina, a significant reduction in the area of β -tubulin III- and pax6-labeled cells was observed in extensively infected regions (arrows). (D-R) Histological sections of central retinal regions from chick embryos electroporated with the indicated DNA constructs plus RCAS-EGFP at E1.5 and incubated for 6 days in vivo. (D, F, H, J, M, P) GFP expression. (E, G, L) Expression of BMP7 detected by in situ hybridization. (K, N, Q) Expression of Collagen IX detected by immunohistochemistry. White arrowheads indicate the immunoreactivity of anti-Collagen IX antibody on the choroid (K, N, Q). (L, O, R) DAPI. Note that the thinning and folding of the retinal epithelium and the ectopic expression of BMP7 and Collagen IX caused by Wnt2b overexpression were suppressed by C-TSKB in vivo. (S) Quantification of the thickness of the retinal layer in retinas electroporated with the indicated DNA constructs. Note that at least four LRR domains are also necessary and sufficient to inhibit the effects of Wnt2b in vivo. Asterisk, $p < 0.01$ based on a two-tailed Student's t-test. Error bars represent the SD. (T) For the in vivo assay, infection of RCAS:Wnt2b with RCAS:LINGO-1-ex ($43 \pm 16 \mu\text{m}$, $n=3$), RCAS:Akhirin ($33 \pm 6 \mu\text{m}$, $n=3$), or RCAS:Equarin ($43 \pm 15 \mu\text{m}$, $n=3$) didn't inhibit Wnt2b activity. Scale bars = $50\mu\text{m}$ in B; $100\mu\text{m}$ in C.

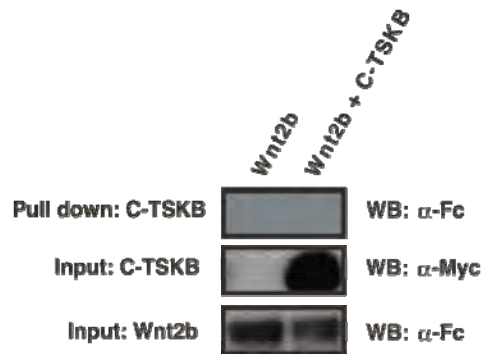
3-1-6: TSK binds to Fzd4 directly.

To investigate the possibility of a biochemical interaction between TSK and Wnt signaling molecules, we next performed co-precipitation assays by transfection of tagged constructs in COS-7 cells (Figure 8A). Wnt2b-Fc pulled down both Flag-tagged Fzd4-CRD [cysteine-rich domain, the site of high-affinity Wnt binding (Bech-Hansen, et al. 2000)] and Flag-tagged Fzd5-CRD (Figure 8B) and also Flag-tagged LRP5-ex (extracellular domain of LRP5) (Figure 8D). When Myc-His-tagged C-TSKB was co-precipitated with Fc-tagged Wnt2b, co-precipitation with nickel-chelating resins did not pull down any protein (Figure 8C). When Fc-tagged C-TSKB was co-precipitated with Flag-tagged LRP5-ex, Flag-tagged Fzd4-CRD or Flag-tagged Fzd5-CRD, co-precipitation with proteinG resins only pulled down Fzd4-CRD (Figures 8D and E). Another isoform of the TSK gene, C-TSKA, which differs in structure of the C-terminus from C-TSKB (Ohta et al., 2006), also pulled down Fzd4-CRD (Figure 8E). To exclude the possibility that binding between C-TSKB and Fzd4 could be detected because of illegitimate interactions in the endoplasmic reticulum of transfected cells, we also performed co-precipitation assays with purified proteins. As shown in Figure 8F, binding between the affinity purified V5-His-tagged mouse TSK (M-TSK) protein (Figure 8G) and purified Fc-tagged mouse Fzd4-CRD (M-Fzd4-CRD) protein (Figure 8H) was also detectable. To confirm that TSK binds to the CRD domain of the Fzd4 receptor, we performed competitive binding assays with Fzd4-CRD, C-TSKB, Wnt2b or Norrin, a highly specific ligand for Fzd4 (Xu Q, et al. 2004). Figure 8I shows that binding of Myc-Flag-tagged Fzd4-CRD with Fc-tagged Wnt2b was inhibited by the addition of Myc-His-tagged C-TSKB protein, whereas Akhirin and Equarin did not interfere with the interaction between Wnt2b and Fzd4 (Figures 8J and K). Furthermore,

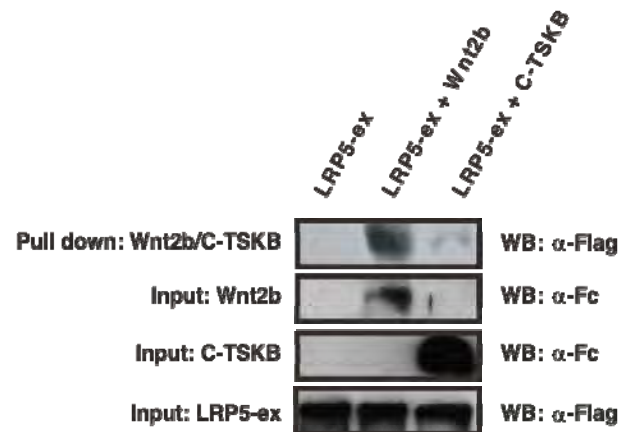
binding of Myc-Flag-tagged Fzd4-CRD with Myc-His tagged C-TSKB was inhibited by Myc-alkaline phosphatase (AP)-tagged Norrin protein (Figure 8L). We next sought to identify specific subdomains of TSK involved in Fzd4 binding and evaluated the binding to Fzd4-CRD of different C-terminally truncated constructs of C-TSKB, containing a variable number of LRR domains. Interestingly, Fzd4-CRD bound to all mutant forms of CTSKB (Figure 8M), indicating that a single LRR is sufficient for the binding of C-TSKB to Fzd4-CRD.



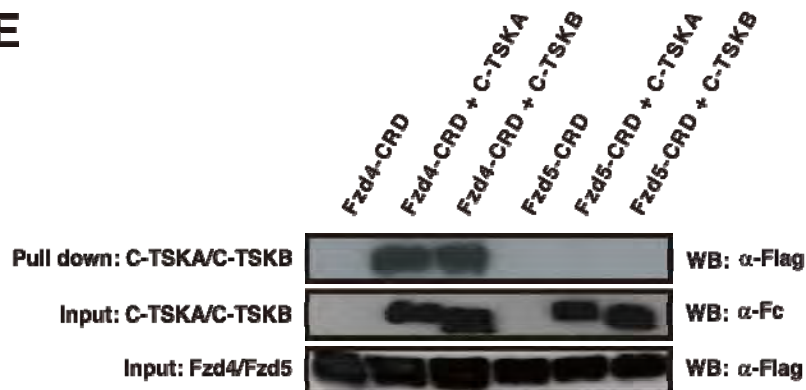
C



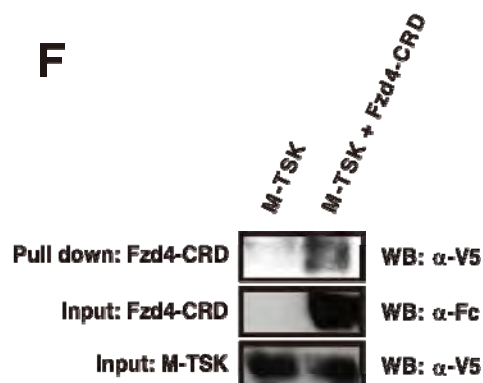
D



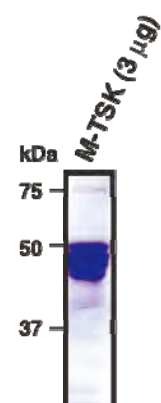
E



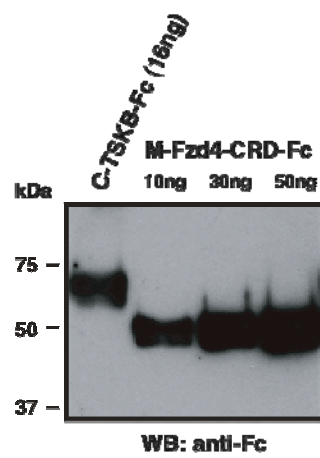
F



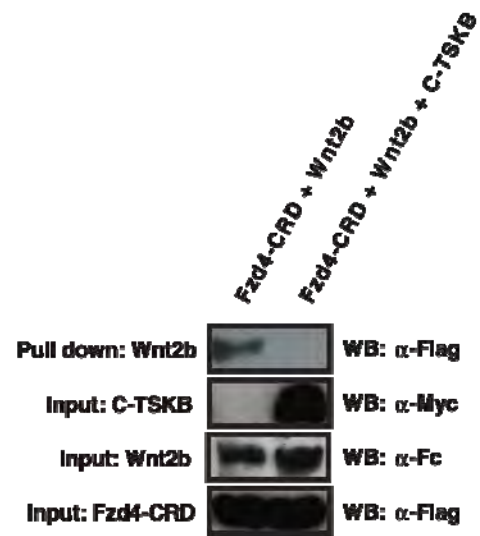
G



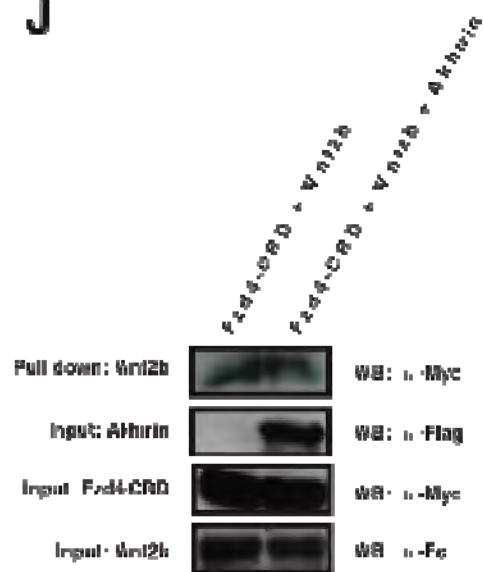
H



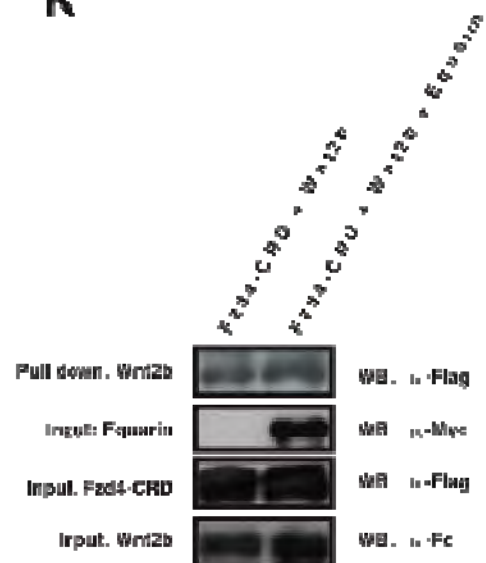
I



J



K



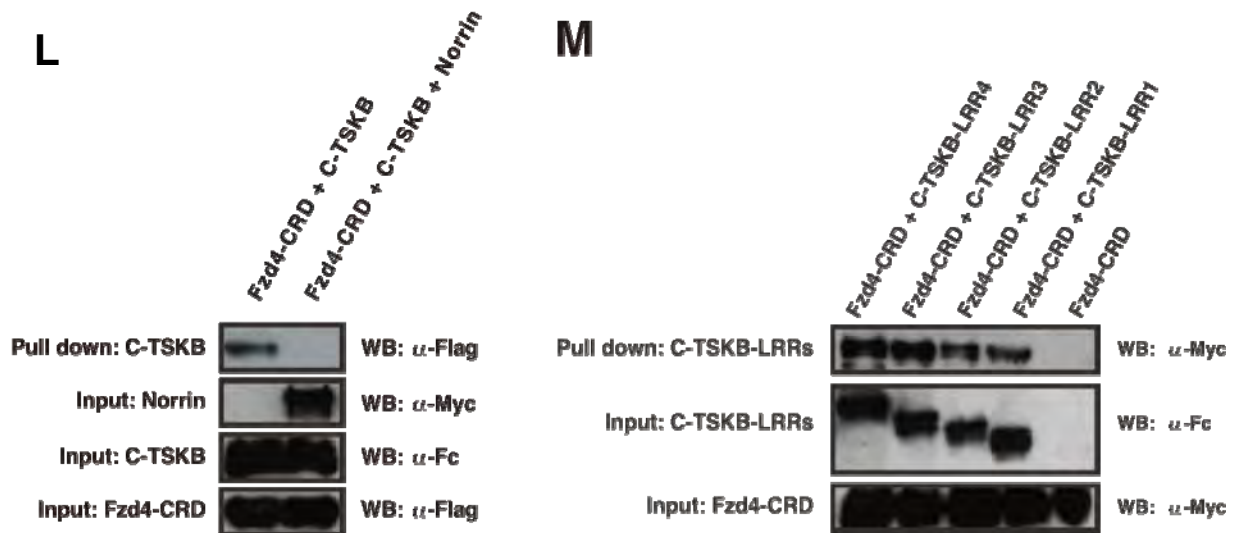
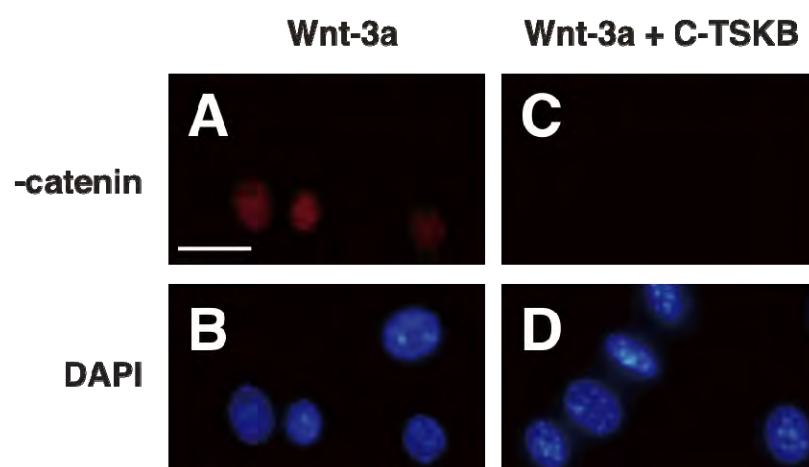



Figure 8. TSK Binds to Fzd4 Directly. (A) The protein blotting data of proteins used in this paper are listed. (B) Coimmunoprecipitation of Wnt2b-Fc and Fzd4-CRD-Myc-Flag or Fzd5-CRD-Myc-Flag. (C) Co-immunoprecipitation of C-TSKB-Myc-His and Wnt2b-Fc. (D) Co-immunoprecipitation of Wnt2b-Fc or C-TSKB-Fc and LRP5-ex-Flag. (E) Co-immunoprecipitation of C-TSKA-Fc or C-TSKB-Fc and Fzd4-CRD-Myc-Flag or Fzd5-CRD-Myc-Flag. (F) Co-immunoprecipitation of purified M-TSK-V5-His and Fzd4-CRD-Fc. (G) Coomassie Blue staining of purified M-TSK-V5-His protein. (H) Quantification of soluble CTSKB-Fc and Fzd4-CRD-Fc proteins. (I) Competition assay of Wnt2b-Fc and C-TSKB-Myc-His for the binding to Fzd4-CRD-Myc-Flag. (J, K) Competition assay. Soluble molecule Akhirin (J) and Equarin (K) did not interfere with the interaction between Wnt2b-Fc and Fzd4-CRD-Myc-Flag. (L) Competition assay of C-TSKB-Myc-His and Norrin-3Myc-AP for the binding to Fzd4-CRD-Myc-Flag. (M) A single LRR domain is sufficient to bind to Fzd4-CRD.

3-1-5: Fzd4 is a TSK receptor


Using immunocytochemistry and immunoblotting, we next examined the effects on the nuclear translocation of β -catenin after Wnt signaling stimulation in L cells expressing Fzd4 (Figure 9F) in the presence or absence of TSK (Figures 9A-E). As previously described, application of Wnt3a protein to L cells induced the translocation of β -catenin into the nuclei (Figures 9A and E), which was not detected when L cells were pretreated with C-TSKB protein (Figures 9C and E). These data are most readily explained by the hypothesis that Fzd4 functions as a receptor for TSK and that TSK inhibits Wnt signaling by competing with Wnt ligands for receptor binding at the cell surface. To further confirm this possibility, we expressed Fzd4 or Fzd5 proteins in COS-7 cells and assayed their binding to TSK-AP, a fusion protein of TSK conjugated with AP. Only Fzd4 expressing COS-7 cells showed specific binding to TSK-AP compared with control COS-7 cells (Figures 9G and H). Calculation of the dissociation constants (Kd) for TSK-AP binding to Fzd4 and Fzd5 yielded affinity values of 2.3×10^{-10} M and 1.4×10^{-9} M, respectively (Figures 9I-K). Moreover, in the presence of Wnt3a protein, binding of TSK-AP protein to Fzd4 was inhibited (Figures 9L and M). All together, these observations strongly suggest that TSK inhibits Wnt signal transduction by interacting directly with Fzd4 at the cell surface and preventing Wnt2b from binding Fzd4 and stimulating receptor activity.

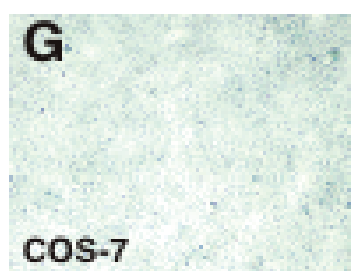


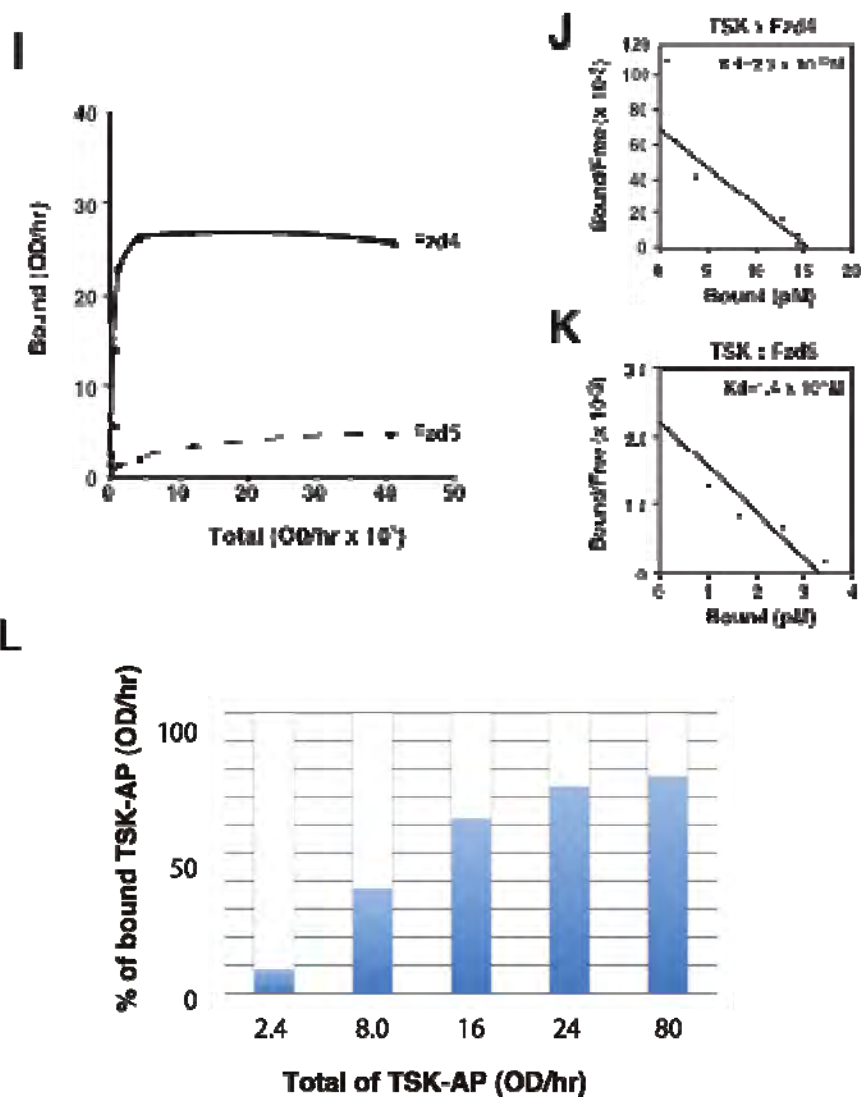
E

Wnt-3a (7ng/ml)	-	+	+	+
human IgG	0	100	0	0
C-TSKB-Fc	0	0	30	100
β -catenin				

F

Fzd4—





M

Applied TSK-AP	Bound TSK	Bound TSK+Wnt3a	% of inhibition
2.4 OD/hr	0.035 OD/hr	0.003 OD/hr	91.4
8	0.131	0.049	62.6
16	0.151	0.094	37.7
24	0.332	0.245	26.2
80	0.394	0.305	22.6

Figure 9. TSK is a Fzd4 Ligand. (A-E) Immunocytochemical (A, C), DAPI staining

(B, D), and immunoblotting (E) analyses of β -catenin translocation into the nucleus in the presence (C-E) or absence (A, B, E) of C-TSKB protein. (F) L cells express Fzd4. (G, H) Binding of C-TSKB::AP to control COS-7 cells (G) and Fzd4-expressing COS-7 cells (H). (I-K) Saturation binding (I) and Scatchard analysis of C-TSKB:AP binding to Fzd4 (J) or Fzd5 (K) expressing COS-7 cells. (L and M) Inhibition of TSK-AP binding with Fzd4 by Wnt3a. (L) The binding of TSK-AP protein to COS-7 cells expressing Fzd4 receptor was observed in the presence (1 μ g/ml) or absence of Wnt3a protein. Blue column shows the % of bound TSK-AP protein to Fzd4 in the presence of Wnt3a. The interaction between TSK-AP and Fzd4 was effectively inhibited by Wnt3a when the applied TSK-AP protein concentration was lower, but not higher.

Scale bars = 20 μ m in A-D.

3-2: Part B

Tskushi regulates neural stem/progenitor cell proliferation in the mouse brain.

3-2-1: TSK expression in the SVZ.

Previously, we found that TSK regulates neural stem cell proliferation in the retinal stem/progenitor cell by controlling Wnt signaling. To check whether TSK could have a role in SVZ neurogenesis in the postnatal and adult brain, I first analyzed the expression of the TSK in the SVZ and DG at P0 to adult stages. The expression of the TSK was detected by LacZ staining in SVZ and DG, where neurogenesis occurs (Figures 10A-I). The high level expression of TSK at SVZ was observed around at P14 (Figure 10E). Although TSK expression was observed in the cortex and striatum as early as P0 and persisted till P14, but it was absent or weak at adult stage (Figures 10B, E, and H). In the SVZ newborn neurons provides interneurons of the OB via rostral migratory stream (RMS) (Figure 10J) (Doetsch and Alvarez-Buylla, 1996; Lois et al., 1996). TSK was also expression in the surrounding region of RMS at different development stages (Figures 10 A, D, G and K). SVZ consists of four types of cells; glial fibrillary acidic protein (GFAP) positive slowly dividing neural stem cell B cell (Doetsch et al., 1997), Mash-1 positive immature precursors cells, C cells generated from B cell, C cell differentiates into doublecortin (DCX) positive migrating neuroblasts A cell differentiated from C cell. Ependymal cell (E cell) formed one cell layer and make the border of lateral ventricle (Figure 10L). To identify the cells that express TSK in the SVZ cells, we performed double immunohistochemistry with antibody against β -galactosidase and SVZ stem cell markers. TSK expression was merged with S-100 β , which is a marker for ependymal cells (Figures 10M-O). These results confirmed TSK expression in the SVZ niche.

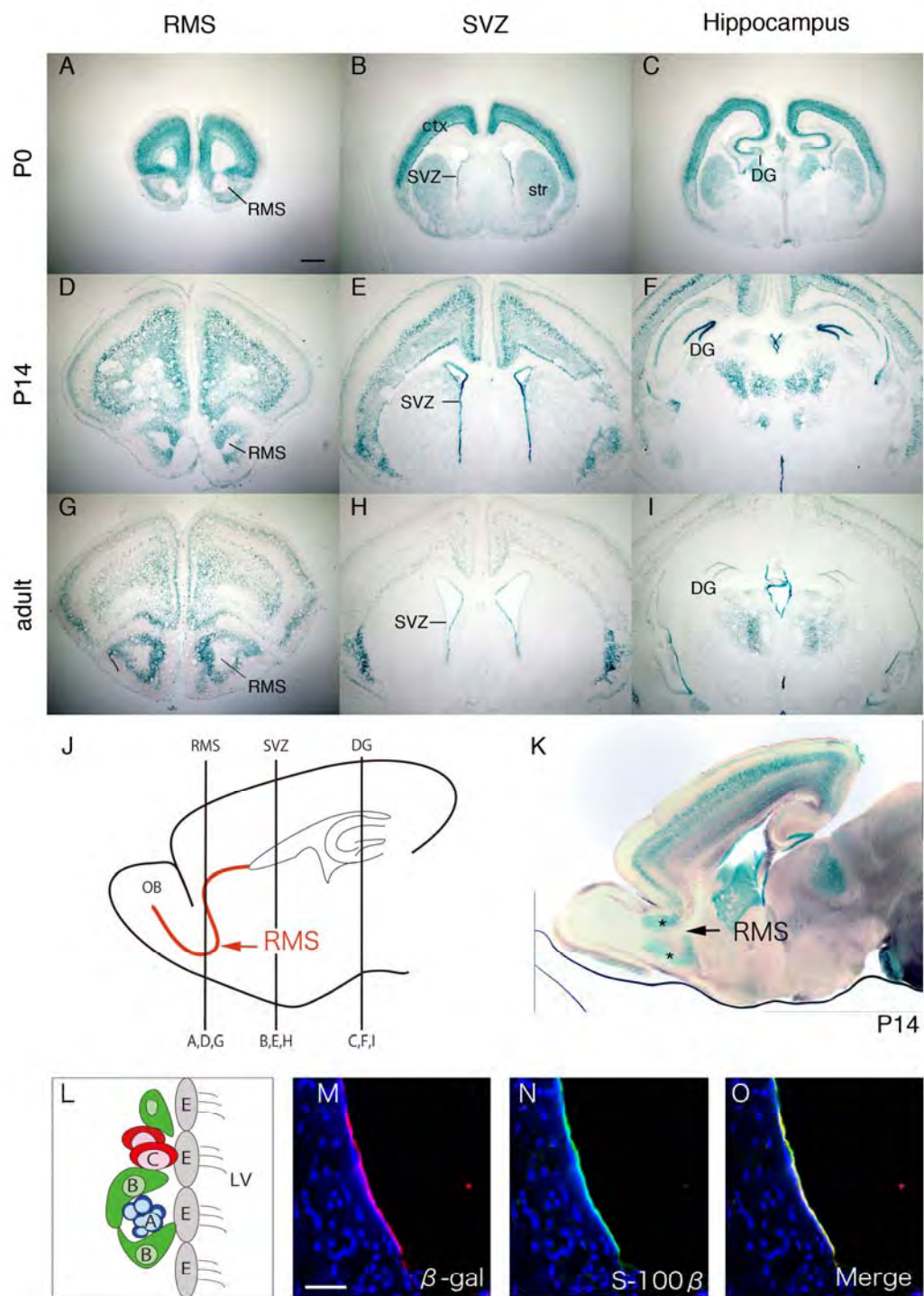
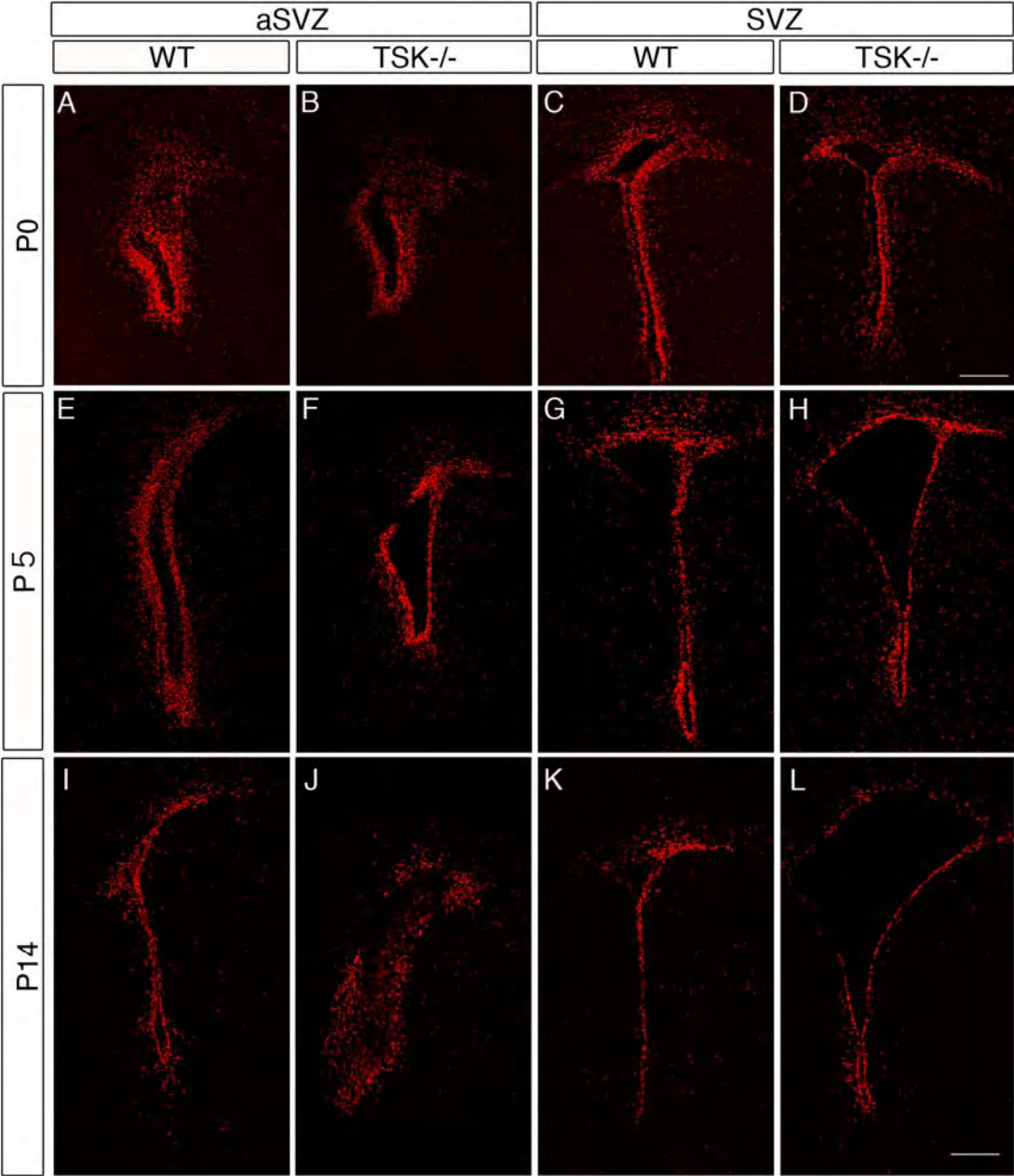


Figure 10. Expression of TSK in the Mouse SVZ and DG. (A-I and K) β -galactosidase staining for TSK expression in coronal section of TSK +/- mouse at P0 (A-C), P14 (D-F), and adult (G-I). (J) Schematic illustration of a sagittal section of mouse brain. The schema showed the migration of neuroblasts along the RMS and vertical lines were identical with coronal section of RMS (A, D, G), SVZ (B, E, H) and DG (C, F, J). Note that TSK was expressed in the SVZ and DG from P0 to adult stages (B, C, E, F, H, I). The expression of TSK was detected in the Ctx and Str at P0 (B) and P14 (E). TSK was expressed in the surrounding area of RMS from P0 to the adult (A, D, G). (K) The sagittal view of the TSK expression at P14. TSK expression was detected in surrounding region of RMS (asterisks) but not on the migrating neuron. (L) Schematic illustration of a coronal section of SVZ. Ependymal cell (E cell, gray) form a single cell layer along the ventricle with astrocytes (B cell, green), transit amplifying cell (C cell, blue) and neuroblasts (A cell, red). (M-O) coronal sections from P14 TSK +/- mice were double-labeled for β -galactosidase (red in M) and S100- β marker of ependymal cell (green in N) in the SVZ. The overlays showed β -gal+/S-100 + cells (yellow in O) in SVZ. SVZ, subventricular zone. RMS, rostral migratory stream. OB, olfactory bulb. DG, dentate gyrus. Ctx, cortex. Str, striatum. Scale bars = 300 μ m in A-I, 50 μ m in M-O

3-2-2: TSK loss affects neural stem/progenitor cells proliferation and the brain size.

Since TSK was expressed in the SVZ in restricted manner, we investigated TSK role in the neural stem cell population in the SVZ-OB system. We analyzed the phenotype resulting from the loss of TSK within the SVZ niche. To evaluate the rate of neurogenesis at the SVZ, I injected BrdU at several stages of WT and TSK^{-/-} mice 30min before killing the mice. As expected, BrdU labeled nuclei were located around SVZ. BrdU⁺ cells were counted within 100 μ m from the surface of LV. At P0 and P5, the number of labeled cells was not significantly different in both TSK^{-/-} and WT (Figures 11A-H and M). In contrast, BrdU⁺ cell number was increased in TSK^{-/-} at

P10-P14 (Figures 11I-L). Despite this increased rate of BrdU incorporation, TSK^{-/-} mouse had large LV. This enlargement was observed from stage at P5 to adult stage (Figures 11D, H, and L). Furthermore, TSK^{-/-} adult brain size was reduced to 10% that of control WT (Figure 12).



M

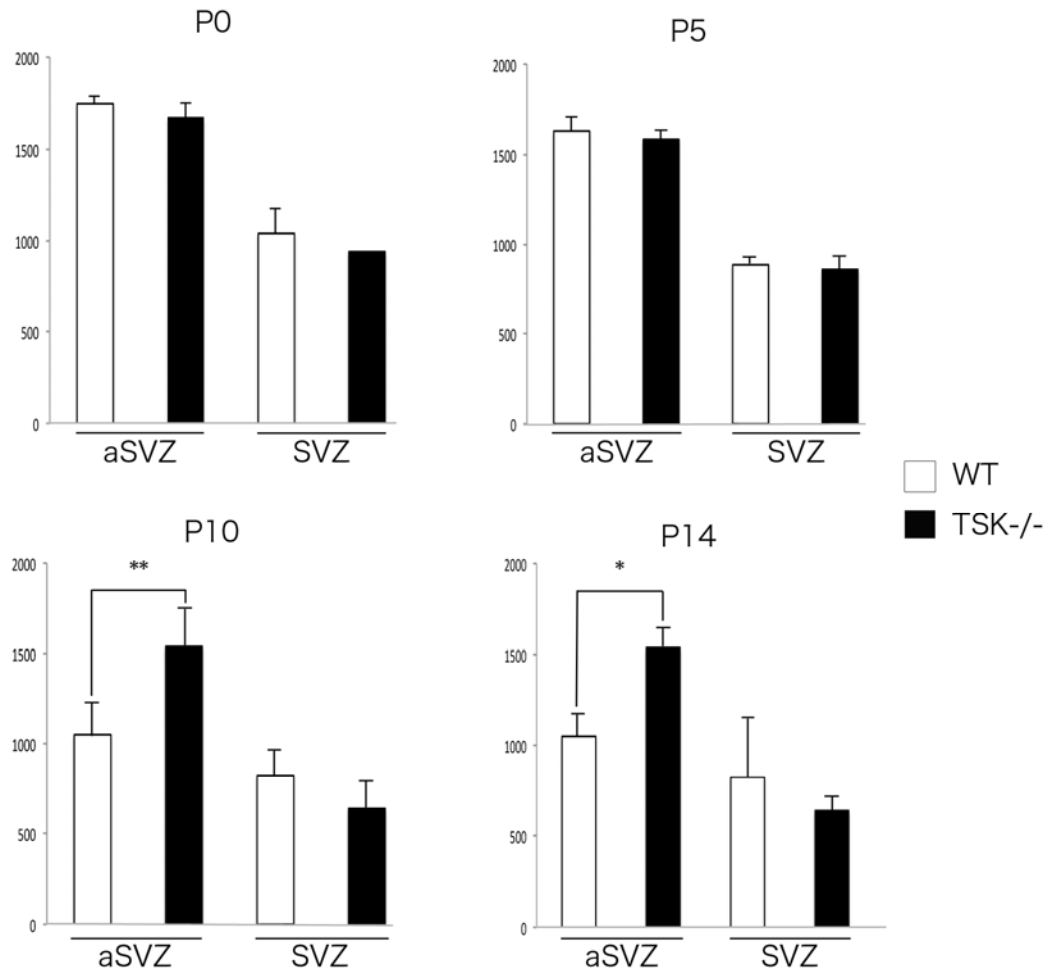


Figure 11. Neurogenesis was Increased in TSK-/- at P10-P14. TSK-/- and WT mice were received single injection with BrdU to label the proliferating cells. (A-L) BrdU staining in coronal sections at the level of aSVZ and SVZ at P0, P5 and P14. aSVZ in WT (A, E, I) and TSK-/- (B, F, J). SVZ in WT (C, G, K) and TSK-/- (D, H, L). (M) Quantification of BrdU-labeled cells in the aSVZ and SVZ. At P10 and P14 neurogenesis in TSK-/- mice were significantly increased at the level of aSVZ. Asterisk, $**P = 0.027$; $*P = 0.016$ based on a two-tailed Student's *t*-test. $n = 3$ mice per group. aSVZ, anterior part of subventricular zone. SVZ, subventricular zone. Scale bars = 300 μ m in D-K and bars = 300 μ m in L.

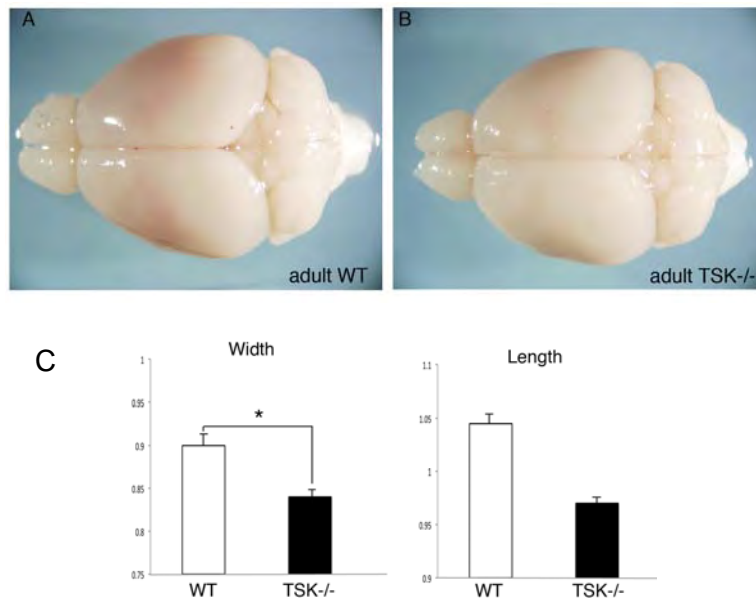


Figure 12. TSK Loss Affected the Brain Size. (A and B) the adult brain were isolated from 2month old WT and TSK-/- . TSK-/- mice brains ($n=10$) showed a reduction in size when compared with control mice ($n=2$) brains. (C) Graphs showed the width and length of cortices from WT and TSK-/- adult mice. Asterisk, $*p<0.001$ based on a two-tailed Student's t -test.

3-2-3: Cell death is increased in the SVZ stem cells around P14.

With the reduction of brain size and enlargement of LV in TSK-/- brain, I observed a considerable amount of cell death in SVZ in TSK-/- . The number of cell death was similar to that of control at P10 (Figures 13A-D, I). Although neurogenesis occurs throughout life in the SVZ niche, the majority of cell death observed within the RMS, where transit amplifying cell and migrating neuroblasts located. I found that there was a marked increase in cell death at P14 of aSVZ (Figures 13E, F) but not SVZ (Figures 13G, H). The increase in cell death in aSVZ at P14 might simply reflect a depletion of newly generated neurons by this time point.

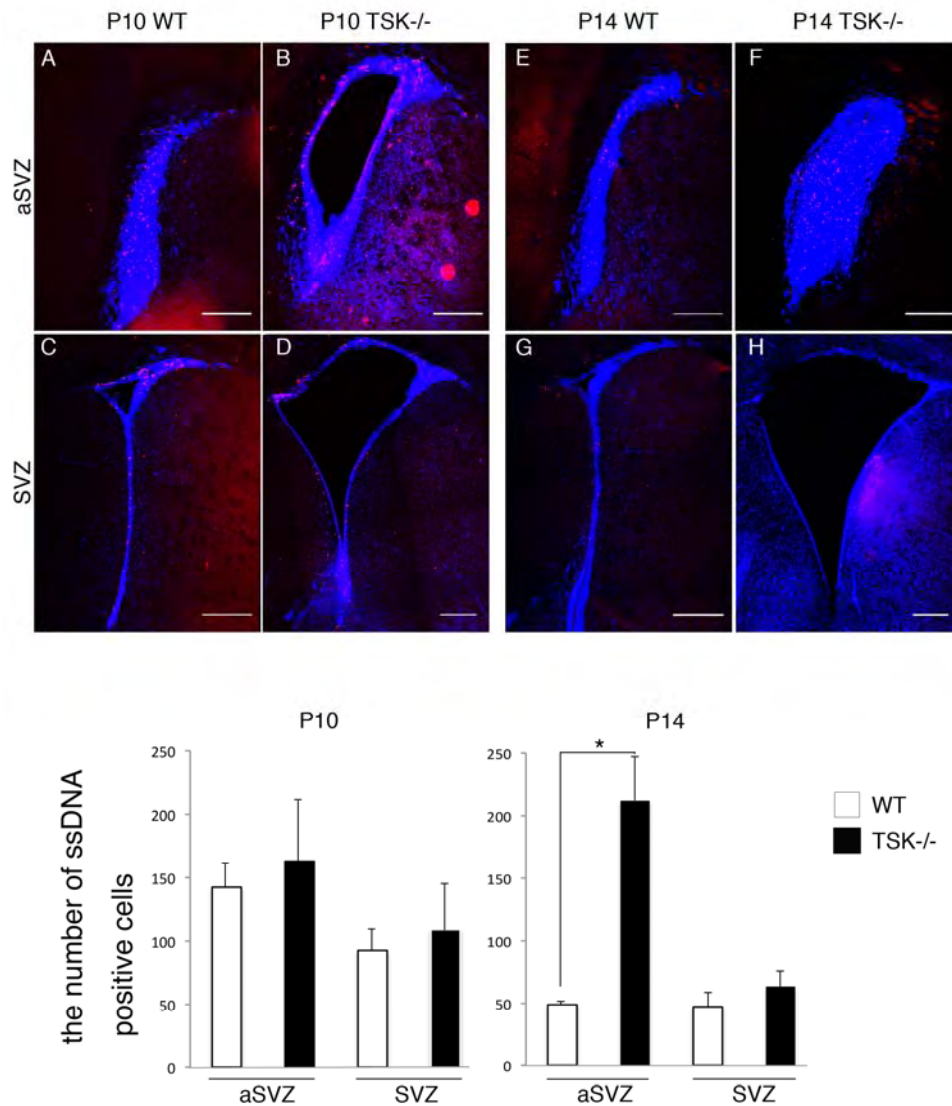


Figure 13. The Cell Death was Increased at P14 of aSVZ. Cell death in SVZ. ssDNA stained nuclei were counted and compared with WT and TSK-/- at P10 and P14. ssDNA positive cell was increased at P14 TSK-/- mouse in aSVZ. Graphs showed the number of ssDNA positive cells increased in the aSVZ at P14 TSK-/- mice. $*P = 0.024$ based on a two-tailed Student's *t*-test. $n = 3$ mice per group. Scale bars = 300 μ m in A- H

3-2-4: TSK deletion led to the expansion of RMS in the aSVZ.

To investigate how TSK is involved in the SVZ neuronal cell lineage during the neurogenesis, we examined the expression of different cell populations in SVZ. We performed IHC using molecular marker of Mash-1 and DCX, a marker for C cell and A cell, respectively. We found that the number of C-cell population was increased in the aSVZ of TSK^{-/-} mice at P10 (Figures 14A-C). In sagittal sections, we observed that the number of DCX positive A cells within the RMS of P14 TSK^{-/-} was higher than that of WT mice (Figures 15A, B). This increment might result in the expansion of RMS in P14 TSK^{-/-} mice. Similarly, DCX positive A cell in aSVZ was increased when the serial coronal sections of the RMS from P14 WT and TSK mice were subjected to DCX staining (Figures 15C-J). This observation is reasonable since the number of C cell from which A cell differentiate were increased in aSVZ of TSK^{-/-} mice (Figures 14A-C).

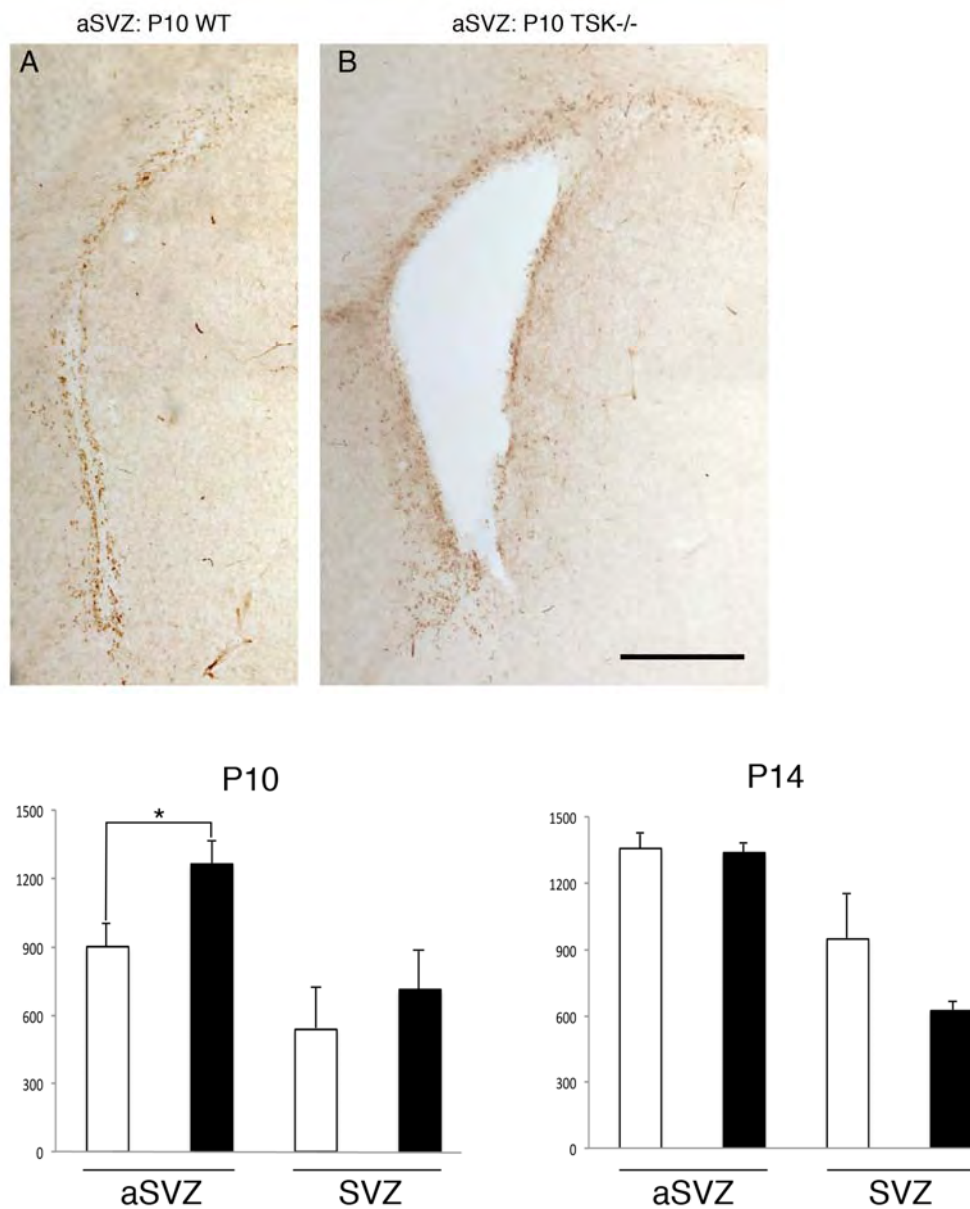


Figure 14. The C Cell Population was Increased in the aSVZ at P10. C-Cell was labeled with Mash-1 antibody. Mash-1+ cells were counted at aSVZ and SVZ in WT (A) and TSK-/- (B). Graphs showed the number of Mash-1 positive cell increased in the aSVZ at P10 TSK-/- mouse. * $P = 0.05$ based on a two-tailed Student's t -test. $n = 3$ mice per group. Scale bars = 300 μ m in A and B.

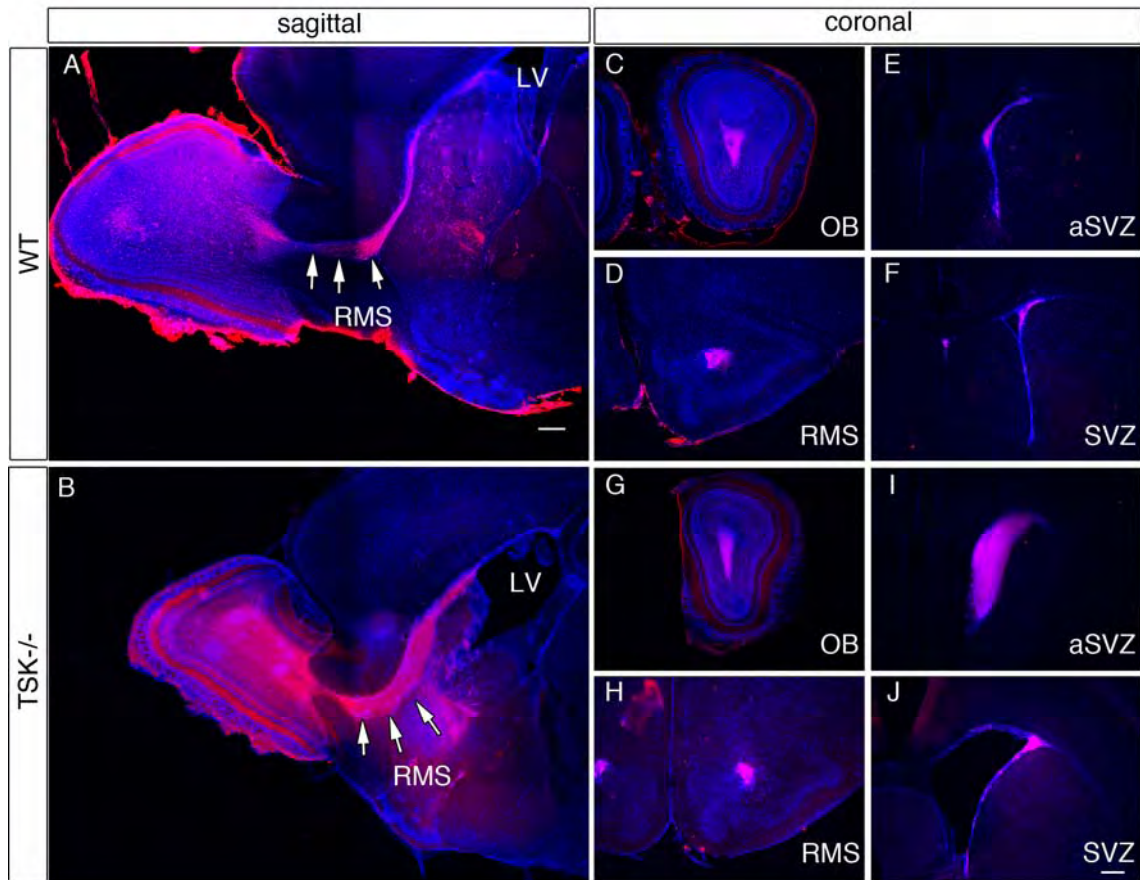


Figure 15. The RMS was Expanded in the TSK-/- at P14. SVZ new born neurons migrate SVZ to the OB along the RMS (A, B white arrow). TSK-/- and WT brain sagittal sections were stained with DCX antibody (A, B). Note the RMS was expanded in TSK-/- compared to the WT. (C-J) P14 TSK-/- and WT coronal sections. The coronal section was observed four different areas within the RMS from anterior to posterior: OB (C, G), RMS (D, H), aSVZ (E, I), and SVZ (F, J). Scale bars = 300μm in A-J.

3-3: Part C

Tsukushi is required for anterior commissure formation in mouse brain

3-3-1 TSK is expressed in the mouse brain

Previously, we reported that TSK is involved in neural development in *Xenopus* (Kuriyama et al., 2006). To address TSK functioning in vivo, we established TSK^{-/-} mice, which were viable and fertile, by replacing the exon with a LacZ/Neo selection cassette (Figure 15). We examined the expression of TSK using β -galactosidase staining of TSK^{+/-} brains from stages E11.5 to P0 (Figure 15). TSK was widely expressed in almost all brain regions at the embryonic stage (Figures 15A and B). At the P0 stage, the expression of TSK was observed in the cortex and the lateral ventricle (Figures 15C and D). The expression of TSK at the adult stage was restricted in the subventricular zone and in the lateral nucleus of the amygdala (Figure 15E). Therefore, TSK expression was widely detected in the brain during development until the adult stage.

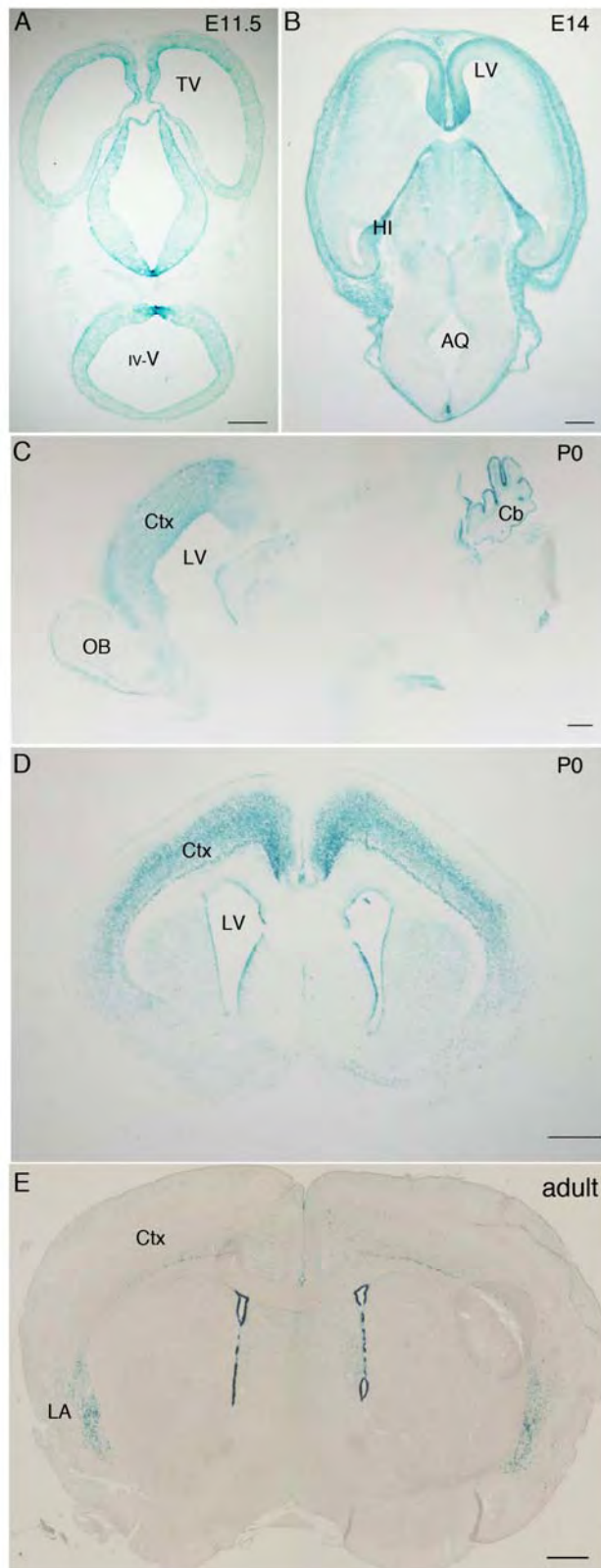


Fig. 15. TSK is expressed in different stages in the mouse brain.

β -galactosidase staining for TSK expression in a horizontal section of TSK +/- mouse embryos at E11.5 (A) and E14 (B). TSK was widely expressed in the brain at embryonic stages. (C, D) TSK expression in the TSK +/- mouse brain on P0 in sagittal (C) and coronal (D) sections. TSK was expressed in the Ctx and Cb at P0. (E) Adult expression of TSK in a coronal section. TSK expression was restricted to the SVZ. TV, telencephalic ventricle; -V, fourth ventricle; LV, lateral ventricle; HI, hippocampus; AQ, Aqueduct. SVZ, subventricular zone. LA, lateral nucleus of the amygdala. Scale bars = 300 μ m.

3-2-2. TSK deletion affects the anterior commissure tract

To start a phenotypic analysis of the TSK^{-/-} brain, we first examined the brain morphology of the TSK^{-/-} brain using HE staining in the adult stage (Figures 16A and B). We found that the AC was defective in the TSK^{-/-} adult brain (Figures 16A and B). To confirm these defects, we performed hematoxylin and KB staining, which are widely used methods for the staining of the myelin sheath of the nervous system. We prepared coronal sections of the adult mouse brains at various levels and compared the AC formation between the WT and TSK^{-/-} brains (Figures 16C-F). The AC is a bipartite tract interconnecting olfactory structures and the anterior piriform cortex and the posterior piriform cortex of the temporal lobes[4]. As shown in Figures 16C-F, the aAC and pAC axons were recognized by KB staining in the WT coronal sections (Figures 16C and E), but the axons of the aAC and pAC were extremely thin in the TSK^{-/-} brain (Figures 16D and F). Furthermore, the pAC failed to cross the midline in the TSK^{-/-} brain (Figures 16F). To quantify these data, we measured the area of the aAC axons (Figures 16G and H). The area of the aAC axons in the TSK^{-/-} brain was almost 5 times thinner than the area of the axons in the WT brain (Figure 16I). This AC axonal absence was observed in almost all of the adult TSK^{-/-} mouse brains (n=20). In addition to these defects in AC formation, we also found that the CC in TSK^{-/-} brains shows a thinner axonal bundle than the WT that might be due to an enlargement of the lateral ventricle (Figures 16E and F).

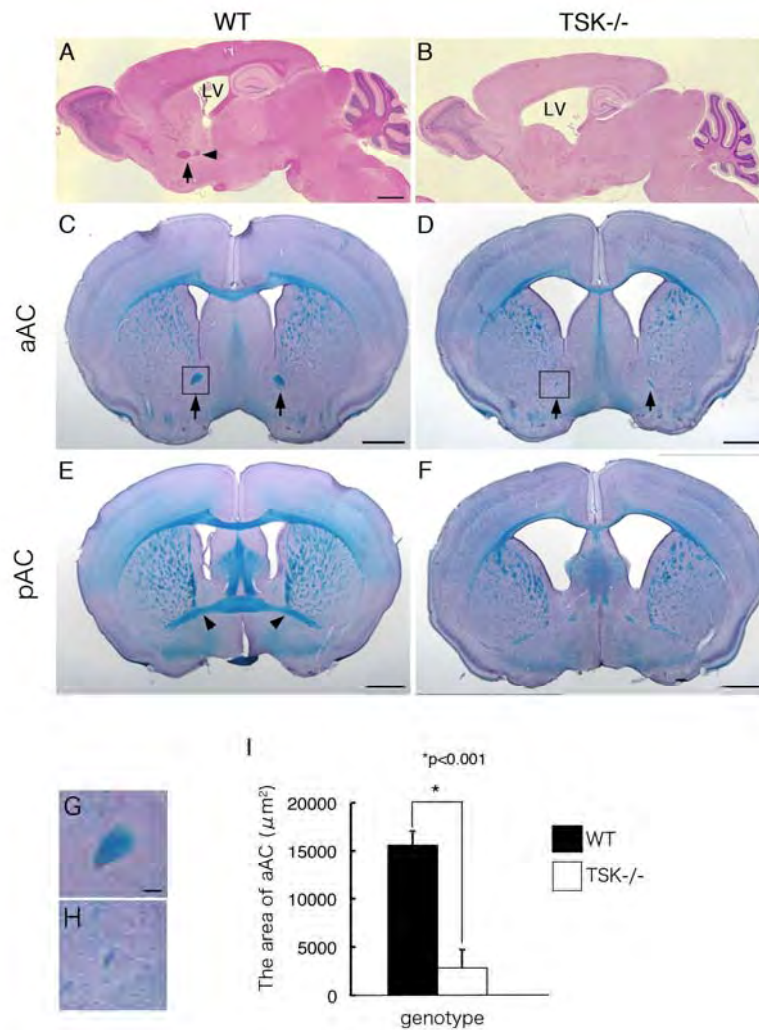


Figure 16. AC Formation is Diminished in the Adult TSK^{-/-} Brain. (A, B) HE staining of sagittal sections in a 2 month old WT (A) and TSK^{-/-} brain (B). (C-F) KB staining for myelinated axons in the adult stage. Coronal section at the levels of the aAC (C, D) and pAC (E, F). Note that the axons of the aAC (arrows) and the pAC (arrowheads) in the TSK^{-/-} brain (D, F) were thinner than the WT (C, E). (G, H) High-magnification of the square areas in (C) and (D). (I) Measurement of the aAC area in the WT and TSK^{-/-} brains. Graph showing the area of the aAC of WT (n=4) and TSK^{-/-} (n=15) mouse brains. Asterisk, *p<0.001 based on a two-tailed Student's *t*-test. Scale bars = 1 mm in A-F, 250 μm in G and H.

3-2-3. TSK is involved in AC formation

To investigate the role of TSK in AC formation, we reconstructed the commissural pathway from serial horizontal sections of WT and TSK^{-/-} brains at the P0 and adult stages and observed the aAC and the pAC pathways (Figure 17). The horizontal serial sections of the WT and TSK^{-/-} adult and neonatal brains were stained with KB and an anti-neurofilament antibody, respectively. In the adult TSK^{-/-} brain, we did not observe any thick AC axons extending from the ventral to the dorsal area compared to the WT brains (Figures 17A and B). On P0, the AC was formed, but the bundle of AC axons was thin and did not cross the midline (Figures 17C and D). The midline crossing AC axons in the P0 TSK^{-/-} brains might be the commissural component of the stria terminalis (Figure 17D) (Jouandet et al., 1983). Moreover, we analyzed AC formation at different neonatal stages, P7 and P10, and found that this thinner bundle of AC axons remained at P7 but was completely diminished at P10 (Figures 17E and F). These data indicate that TSK is required for AC formation in the mouse brain.

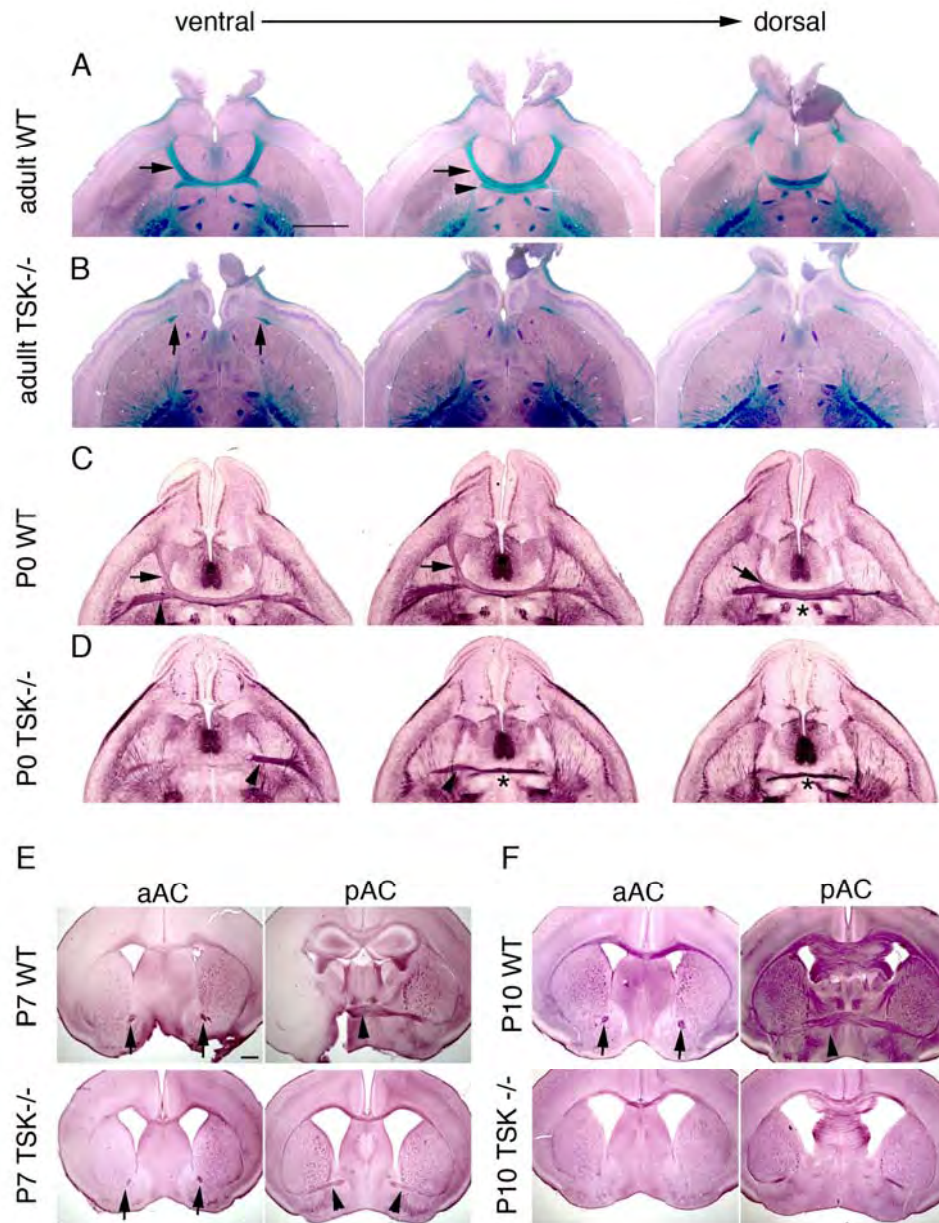


Figure 17. TSK is Required for Normal AC Formation. (A, B) AC axons in serial horizontal sections were stained with KB in WT (A) and TSK^{-/-} (B) adult brains. Fibers of the aAC (arrow) elongate from the AON and cross the midline with pAC (arrowhead). A thin aAC was observed in the TSK^{-/-} brain (arrow in B). (B) Midline crossing axons were not observed in the TSK^{-/-} brain. (C, D) Immunostaining for neurofilament in adjacent slices of WT and TSK^{-/-} brains at P0. In the TSK^{-/-} brain, the aAC was not visible and the pAC (arrowhead) was formed but did not cross the midline. Midline crossing fibers were of the stria terminalis (St) (asterisk). (E, F) Coronal section of

TSK^{-/-} brains from P7 and P10. Note the abnormal formation of the aAC and the pAC at both stages. Arrows and arrowheads indicate the aAC and pAC axons, respectively. Note that the aAC and pAC axons in the TSK^{-/-} adult brain are grossly diminished. Scale bars = 1 mm in A-D, 250 μ m in E and F.

3-2-4. aAC axons do not cross the midline

To further confirm the above defects, aAC axons were traced by an injection of DiI into the olfactory bulb on P2, and DiI-labeled axons were analyzed in horizontal sections on P3. As shown in Figure 18A, DiI-labeled aAC axons grew out of the AON, where the cell bodies of the aAC axons are located, and crossed the midline toward the contralateral side in the WT brain. Although the aAC axons of the TSK^{-/-} brain also grew out of the AON, they do not cross the midline (Figures 18B-D).

To check whether TSK influences the formation of the AC tract, we analyzed the expression pattern of TSK in the developing AC on E15. In the WT brain, the aAC fibers started to elongate toward the midline region on E13.5 and intersect with the contralateral AC fibers in the midline on E14.5 to E15 (Uemura et al., 2006). The immunostaining of horizontal sections of the E15 TSK^{+/-} brains with anti-L1 and anti- β -galactosidase antibodies showed that TSK was expressed in the midline of the brain adjacent to the pAC and the AON on E15 (Figures 18E and F) but not in the aAC and pAC axons themselves (Figures 18E-H). This expression of TSK was maintained in the P0 and P7 brains (Figures 18G and H). To address whether TSK was expressed in the cell bodies of the AON neurons, we injected DiI into the AON and traced the cell bodies of the AON retrogradely (Figures 18J and M). As previously reported (Uemura et al., 2006), the retrogradely labeled cells expressed calbindin, a marker of AON cells (Figures 18I-L). We found that the expression of TSK overlapped with the cells labeled

by DiI (Figures 18M-P). These results confirmed TSK expression in the AON and the surrounding area in the route of AC axons from developmental to postnatal stages and suggest the involvement of TSK in AC formation.

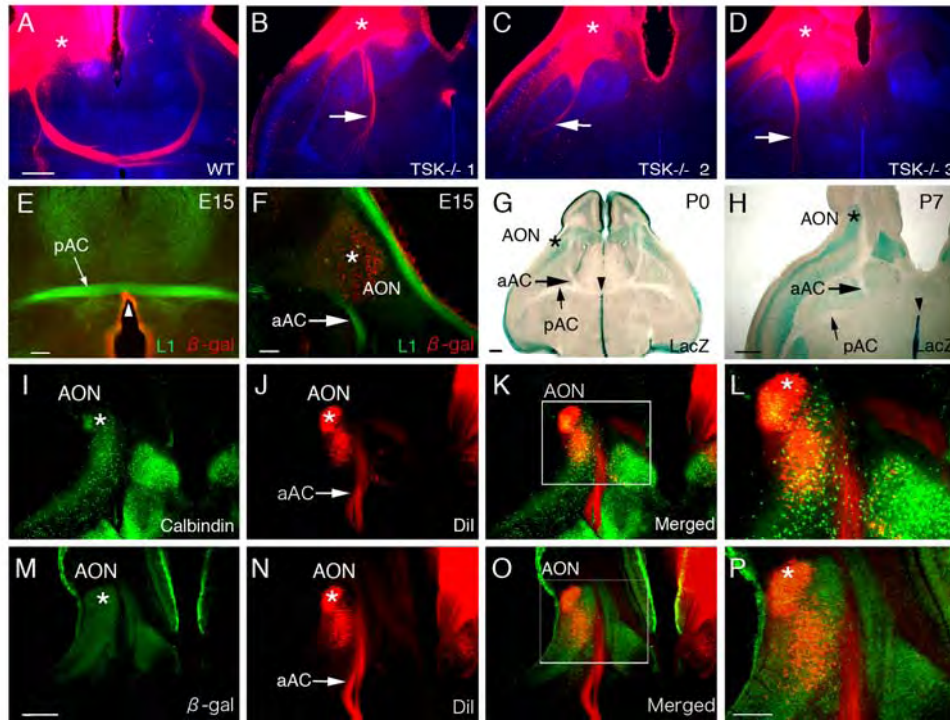


Figure 18. The aAC Axons Never Cross the Midline in the TSK^{-/-} Brain. (A-D) DiI was injected into the olfactory bulb on P2 and the aAC axons were observed horizontally on P3 in WT brains (A) and in three different samples of TSK^{-/-} brains (B-D). DiI-injected sites in the olfactory bulb are indicated by asterisks. Arrows point to the misguided axons (B-D). Note that the pattern of misrouting varied among the mutant mice. (E, F) immunostaining with antibodies against β -galactosidase (red) and L1 (green) was performed on horizontal sections in E15 TSK^{+/-} brains. (E) TSK-expressing cells were located in the midline (white arrowhead). (F) TSK expression was observed in the AON (white asterisk). (G, H) β -galactosidase staining of the TSK ^{+/-} brain was performed in horizontal vibratome sections on P0 (G) and P7 (H). The expression of TSK was observed in the AON area (asterisk) and the midline

(arrowhead). (I-L) The population of calbindin-positive cells in the DiI retrogradely labeled AON. (J) DiI was injected into the olfactory bulb on P5 and the aAC axons were observed horizontally on P7 in the TSK^{+/-} brain. (K) Calbindin positive cells overlapped with the retrograde DiI labeled cells. (L) High magnification of the white square area in K. (M-P) TSK expressing cells in the DiI retrogradely labeled AON (red). (M) TSK was widely expressed in the AON (asterisk) and in the surrounding area of the AC axon (green). (N) Cells in the AON (asterisk) were retrogradely labeled with DiI. (O) Some population of TSK expressing cell overlapped with DiI positive cells. (P) High magnification of the white square area in O. Scale bars = 500 μ m in A-D, 100 μ m in E and F, 300 μ m in G-P.

4. Discussion

4-1: Part A and Part B

In mammals and other warm-blooded vertebrates, several studies have identified a number of different cellular sources of neural stem/progenitor cells within the adult eye (Perron and Harris, 2000; Boulton and Albon, 2004; Ohta et al., 2008). The CB is a neuroepithelial derivative and anatomically located at the most distal tip of the neural retina (Morrison et al., 1996). The CB contains a quiescent population of cells that can form retinal spheres regardless of growth factor condition and differentiate into all types of neural cells, including photoreceptor cells and Müller glia (Ahmad et al., 2000; Tropepe et al., 2000). Increasing evidence has pointed to Wnts as potential extrinsic regulators in the context of the CM development in the eye because the expression of Wnt2b and other additional molecules of the Wnt pathway are detected in overlapping or exclusive patterns in CM in several species (Van Raay and Vetter, 2004; Cho and Cepko, 2006; Liu et al., 2006). In the chick retina, the ciliary margin zone retina contains high levels of LEF that co-localizes with progenitor markers. Overexpression of Wnt2b in the central retina suppresses neuronal differentiation, and blocking Wnt signal with a dominant-negative LEF1 protein inhibits cell proliferation at the CM (Kubo et al., 2003). Further, retinal progenitor cells prolong their proliferative period in vitro in the presence of Wnt2b (Kubo et al., 2003). A recent comprehensive study using mouse retina has described that the expression of Wnt2b and Fzd4 were maintained in mouse CB from embryonic to adult stages (Liu et al., 2003). Further, the activation of TCF/Lef-LacZ, a canonical Wnt reporter transgene, is observed in the CB in postnatal and adult eye (Liu et al., 2003; Liu et al., 2006). Study with retinal sphere also indicates that Wnt3a promotes proliferation of retinal stem/progenitor cells in vitro (Inoue et al.,

2006). Cre-mediated conditional expression of stabilized β -catenin in vivo induced an expansion of the CM, while Cre-mediated inactivation of β -catenin reduced CM gene expression and resulted in aberrant CB development (Liu et al., 2007). Thus, TSK, Wnt2b, and Fzd4 may be involved in the maintenance of an undifferentiated retinal stem/progenitor cells at the CB.

Using chick embryos, we could show that TSK inhibits Wnt signaling in both in vivo and in vitro assays. However, we had concerns about the considerable controversy with respect to the neurogenic and proliferative effects of the Wnt pathway in chick retina because the two different assays in vitro (Kubo et al., 2003) and in vivo (Cho & Cepko, 2006) showed the very different results. Kubo et al. (2003) demonstrated an increase in proliferation of Wnt-2b expressing explants in vitro, whereas Cho & Cepko (2006) showed that the level of proliferation in vivo in Wnt-2b infected central retinal area was lower than that of the normal uninfected central retina. Then, we have performed the same in vivo and in vitro assays to reconcile these disparate effects, and found that both results obtained by these different assays were true. We clearly demonstrated a dramatic hyperproliferation of Wnt2b-expressing explants in vitro. We also showed the ectopic induction of a retinal peripheral marker collagen type IX in Wnt2b-infected explants (Figure 6). One plausible explanation for these observations is that the expression of collagen type IX and hyperproliferation are due to the acquisition of stem cell behavior. As Wnt2b-expressing explants demonstrated a high degree of proliferation in vitro, it is possible that retinal cells exposed to a high level of Wnt2b normally in the periphery in vivo are induced to form stem cells. Alternatively, it is possible that some other aspect of the in vitro culture environment enhances proliferation in response to Wnt signaling. We also examined the effect at E7.5 after

infection with retrovirus expressing Wnt2b at stage 10, and didn't find the induction of proliferation in vivo (Figure 7). While collagen type IX was induced in the Wnt2b-infected central retina, additional factors might be needed for such an induction of proliferation in vivo. Alternatively, there might be an inhibition of this role of Wnt in vivo. TSK is expressed in the central retina and may function as a Wnt signaling inhibitor in vivo. Cho & Cepko (2006) suggested that the different results between in vivo and in vitro is their use of constitutive active form of β -catenin (CA- β -catenin). However, we could reproduce their results using Wnt2b (Figures 6 and 7), indicating that the different results between in vivo and in vitro is not due to the difference between CA- β -catenin and Wnt2b. These discrepant effects of Wnt signaling might reflect experimental differences in the timing, duration, and intensity of Wnt signaling. It is also plausible that there are regional and temporal differences in the outcome of Wnt signaling in the developing eye. Further work will be required to elucidate the precise role of Wnt2b in chick eye development.

Since retinal stem/progenitor cells respond to growth factor treatment by extensive proliferation in vivo and in vitro, they are considered to be a potential source of stem cells to support retinal regeneration and may contribute to retinal cell transplantation therapy. However, the molecular mechanisms that maintain and confine quiescent retinal stem/progenitor cells in the periphery of the adult normal retina are still unclear. The failure of neural stem cells in the mammalian and avian retina to renew retinal cells in the postnatal period suggests that retinal stem/progenitor cells find themselves in an inhibitory environment. Recently, it has been reported that biglycan and fibromodulin, which belongs to SLRP family, compose of a unique niche for termed tendon stem/progenitor cells (TSPCs) and control the fate of tendon TSPCs (Bi et al., 2007).

Our results indicate that TSK, which is also a member of SLRP family, directly binds to the Fzd4 receptor expressed in retinal stem/progenitor cells, and restrains their proliferation by inhibiting Wnt signaling in the extracellular space. In the absence of TSK function, retina progenitor/stem cells show a marked increase in their proliferative abilities both in vivo and when cultured in vitro. While these findings expand our knowledge on the molecular control of retinal stem/progenitor cell proliferation and self-renewal, they may also have important implications for the understanding of eye diseases and for the development of clinical applications of retinal stem cells. In particular, it will be important to test whether mutations in the TSK gene are present in eye diseases due to abnormal proliferation, such as different forms of eye tumours. It will also be very interesting to test whether TSK mutant retinas show increased ability for regeneration, and whether retinal stem cell lines could be more efficiently derived and propagated from TSK-deficient retinas.

4-2: Part C

Mice deficient in several key guidance molecules [Netrin (Serafini et al., 1996), Semaphorin (Falk et al., 2005), Eph (Ho et al., 2009), Draxin (Islam et al., 2009), and the FGF receptors (Tole et al., 2006)] have also shown aberrant AC formation, suggesting that the combinational guidance effect of these chemoattractants and chemorepellants plays a crucial role in the formation of the AC axonal tract. These molecules are expressed either in AC axons or in the surrounding regions of the AC axons. Our data demonstrated that TSK was expressed in strategic regions, such as the AON, the regions surrounding AC axons, and in the midline of the brain adjacent to the AC pathway, that have been implicated as the sources of known guidance molecules

(Lindwall et al., 2007). TSK may interact with the above guidance molecules or their receptors directly and modulate their activity.

Midline populations, including the glial wedge, glia of the indusium griseum, and midline zipper glia, play an important role in forebrain commissure formation (Lindwall et al., 2007). These glial cells secrete guidance cues, including Slits (Erskine et al., 2000), Wnt (Keeble et al., 2006), and draxin (Islam et al., 2009), and form cellular boundaries that surround the corpus callosum axonal tract. Similarly, glial cells form a molecular tunnel in the AC pathway and play a crucial role in AC formation (Figure 18, Chénot and Richards) (Islam et al., 2009; Lent et al., 2005). These glial cells secrete not only guidance cues but also extracellular matrix components (ECM) proteins. Previous studies have indicated that heparin sulfate proteoglycans (HSPGs), one of the ECM proteins, interacts with multiple growth factors, such as Shh, FGF and Wnt, and contributes to cortical development (Shimogori et al., 2001; Gunhaga et al., 2003; Viti et al., 2003). Mutant mice bearing a targeted disruption of the heparin sulfate (HS) modifying enzyme, *Ndst1*, showed severe developmental defects of the forebrain, including the AC (Grobe et al., 2005). Moreover, genetic deletion of the HS-polymerizing enzyme, *Ext1*, caused severe guidance errors in the major commissural tracts (Inatani et al., 2003). Based on these studies, it is plausible that the ECMs and proteoglycans trap and incorporate the diffusible proteins and thereby stabilize the diffusible gradients, which is essential for the proper formation of the forebrain commissure. Because TSK belongs to the SLRP family, TSK may interact with other guidance cues and/or ECMs and modulate their function, resulting in an abnormal distribution of the prominent guidance cues. Whatever the mechanisms, the results obtained in the present in vivo analysis emphasize the role of TSK in AC

formation in the mouse brain.

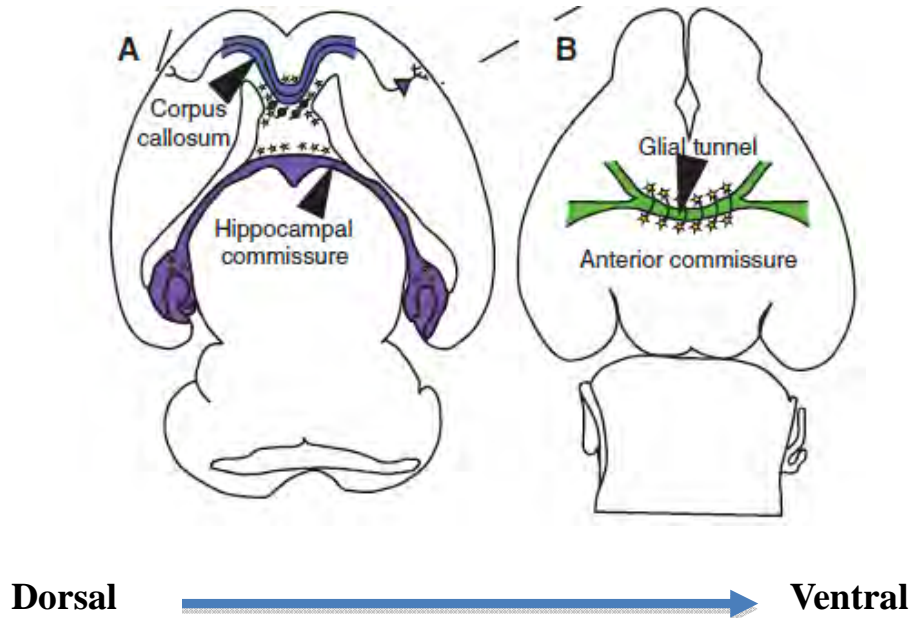


Figure 19. Commissural and Longitudinal Projection in the Forebrain. (A, B) Both glial and neuronal structures are associated with axonal tract in the brain. Depict commissural tracts in schematics of horizontal sections from dorsal to ventral. Associated with the corpus callosum (blue tract in A) are glial wedge and indusium griseum glia and the sling cells. Glia are also associated with hippocampal commissure (purple tract in A) anterior commissure (green tract in B) Midline glial cells form a molecular tunnel in the anterior commissure pathway and play a crucial role in AC formation. TSK was expressed in the midline glia of anterior commissure tract.

5. Conclusion

5-1: Part A

We have previously reported that TSK interacts with and modulates activities of Notch ligand Delta (Kuriyama et al., 2006) and FGF8 (Morris et al., 2007) in addition to the TGF- β family members (Ohta et al., 2004; Ohta et al., 2006). Our new finding in this study is that TSK can function as Wnt signaling inhibitor at the extracellular region by direct binding to Fzd4-CRD, the site of Wnt binding. First, the overexpression analyses using chick embryos in vitro and in vivo clearly demonstrated that TSK possessed the inhibitory activity for Wnt signaling. Second, biochemical assays showed that TSK directly binds to Fzd4-CRD and inhibits the molecular interactions of Fzd4 with Wnt2b or Norrin, which is a highly specific ligand for Fzd4 (Xu et al., 2004). Finally, scatchard analyses of TSK-AP indicated the binding affinity to Fzd4 was 2.3×10^{-10} M. Taken together, our data indicates that TSK is a Fzd4 ligand and TSK inhibits Wnt signaling by direct binding to the CRD of Fzd4 extracellularly. Taken together, our data indicate that TSK is a novel Wnt signaling inhibitor that competes with Wnt2b ligand for Fzd4 receptor binding and controls peripheral eye development.

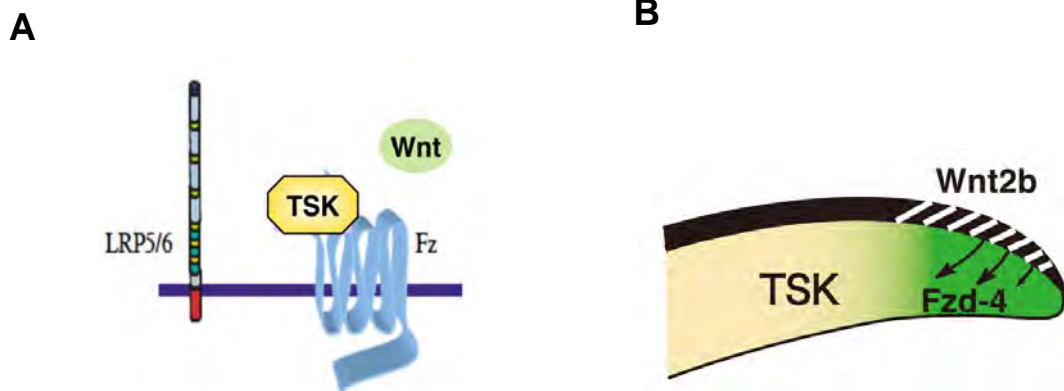


Figure 20. TSK Inhibited Wnt Signaling and Regulate Retinal Stem/Progenitor Cells Proliferation. (A) Schematics of the TSK binding with Frizzled-4 CRD domain and inhibited Wnt activity at the extracellular region. (B) TSK (yellow), Frizzled-4 (green), Wnt2b (black and white) expression in the CMZ chick retina.

5-2: Part B

TSK was expressed in SVZ and DG where neurogenesis occurs from P0 to the adult stage. The high level expression of TSK at SVZ was observed around P14. TSK was expressed in the ependymal cells in the SVZ cells niche. BrdU labeling analysis showed that cell proliferation was increased in TSK^{-/-} brain at P14, though the number of cell death was also increased in TSK^{-/-} brain at P10-P14. Among four different kinds of cells located at neuronal niche area in the SVZ, I found that the cell proliferation of C and A cells were increased at aSVZ and the RMS was extremely expanded in TSK^{-/-} brain.

5-3: Part C

TSK was expressed in strategic regions, such as the AON, the regions surrounding AC axons, and in the midline of the brain adjacent to the AC pathway from embryonic to the adult stages and AC formation in the TSK^{-/-} adult brain was diminished. Our immunohistochemical study showed that the aAC and pAC axons never crossed the brain midline. Furthermore, the DiI labeling technique demonstrated the misguidance of the aAC axons, although they grew out of the AON. Therefore, our data indicate the involvement of TSK in the navigation of AC axons.

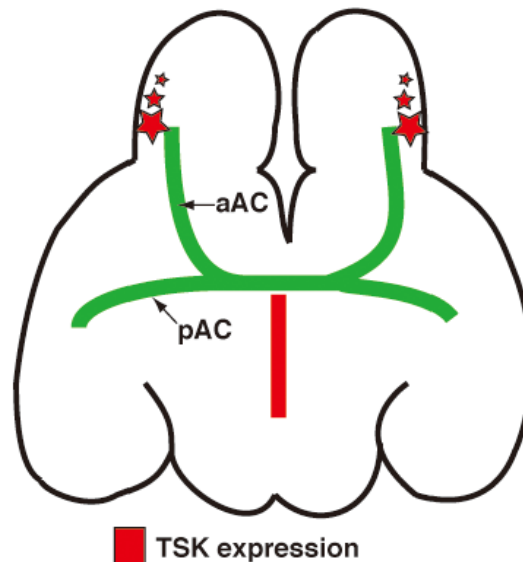


Figure 21. TSK was Expressed Surrounding AC Axonal Tract. TSK was expressed AON (red stars) and midline of the AC pathway. AC axons of TSK^{-/-} brain never cross the midline.

5-4: final conclusion

In early embryogenesis, TSK directly interact with BMP, Notch and FGF8 and involved in the morphogenesis. Our study reveals a new role of TSK in the CNS, we show that TSK regulate Wnt activity by interact with Wnt receptor of Frizzled. TSK regulates neural stem/ progenitor cell proliferation in the CNS. And also TSK involved in the Axonal guidance. TSK may interact and regulate guidance molecules. Our data indicate that, TSK plays an important role in the coordination of signaling balance at the extracellular region.

References

Ahsan M, Ohta K, Kuriyama S, & Tanaka H (2005) *Novel soluble molecule, Akhirin, is expressed in the embryonic chick eyes and exhibits heterophilic cell-adhesion activity.* Dev Dyn 233 : 95-104.

Boulton, M., and Albon, J. (2004). *Stem cells in the eye.* Int J Biochem Cell Biol 36: 643-657.

Coles, B.L., Angenieux, B., Inoue, T., Del Rio-Tsonis, K., Spence, J.R., McInnes, R.R., Arsenijevic, Y., and van der Kooy, D. (2004). *Facile isolation and the characterization of human retinal stem cells.* Proc Natl Acad Sci U S A 101 : 15772-15777.

Chenn, A., and Walsh, C.A. (2002). *Regulation of cerebral cortical size by control of cell cycle exit in neural precursors.* Science 297 : 365-369.

Chen, A., and Walsh, C.A. (2003). *Increased neuronal production, enlarged forebrains and cytoarchitectural distortions in beta-catenin overexpressing transgenic mice.* Cereb Cortex 13: 599-606.

Cho SH & Cepko CL (2006) *Wnt2b/beta-catenin-mediated canonical Wnt signaling determines the peripheral fates of the chick eye.* Development 133:3167-3177.

Dhawan RR & Beebe DC (1994) *Differential localization of collagen type IX isoform messenger RNAs during early ocular development.* Invest Ophthalmol Vis Sci 35:470-478.

Doetsch, F., Alvares-Buylla, A., (1996) *Network of tangential pathways for neuronal migration in adult.* Proc. Natl. Acad. Sci. U.S.A 98: 12796-12801

Doetsch F, Garcia-Verdugo JM, Alvarez-Buylla A (1997) *Cellular composition and three-dimensional organization of the subventricular germinal zone in the adult mammalian brain.* J Neurosci 17:5046-5061

Eriksson, P.S., Perfo;oeva, E., Bjork-Eriksson, T., Aldorn, A.M., Nordborg, C., Peterson, D. A., Gage, F. H., (1998) *Neurogenesis in the adult human hippocampus.* Nat. Med. 4: 1313-1317.

Erskine, L. Williams, E.S. Brose, K. Kidd, T. Rachel, R.A. Goodman, S.C. Tessier-Lavigne, M. Mason, A.C. (2000) *Retinal ganglion cell axon guidance in the*

mouse optic chiasm: expression and function of robos and slits. J Neurosci 20: 4975-4982.

Falk, J. Bechara, A. Fiore, R. Nawabi, H. Zhou, H. Hoyo-Becerra, C. Bozon, M. Rougon, G. Grumet, M. Puschel, W.A. Sanes, R.J. Castellani, V. (2005). *Dual functional activity of semaphorin 3B is required for positioning the anterior commissure.* Neuron 48: 63-75.

Fukuchi-Shimogori, T. Grove, A.E. (2001) *Neocortex patterning by the secreted signaling molecule FGF8.* Science 294: 1071-1074.

Grobe, K. Inatani, M. Pallerla, R. S. Castagnola, J. Yamaguchi, Y. Esko, D.J. (2005) *Cerebral hypoplasia and craniofacial defects in mice lacking heparan sulfate Ndst1 gene function.* Development 132: 3777-3786.

Gunhaga, L. Marklund, M. Sjodal, M. Hsieh, C.J. Jessell, M.T. Edlund, T. (2003) *Specification of dorsal telencephalic character by sequential Wnt and FGF signaling.* Nat Neurosci 6: 701-707.

Ho, K.S. Kovacevic, N. Henkelman, M.R. Boyd, A. Pawson, T. Henderson, T.J. (2009). *EphB2 and EphA4 receptors regulate formation of the principal inter-hemispheric tracts of the mammalian forebrain.* Neuroscience 160: 784-795.

Hocking, A.M., Shinomura, T., and McQuillan, D.J. (1998). *Leucine-rich repeat glycoproteins of the extracellular matrix.* Matrix Biol 17: 1-19.

Inatani, M. Irie, F. Plump, S.A. Tessier-Lavigne, M. Yamaguchi, Y. (2003) *Mammalian brain morphogenesis and midline axon guidance require heparan sulfate.* Science 302: 1044-1046.

Inoue, T., Kagawa, T., Fukushima, M., Shimizu, T., Yoshinaga, Y., Takada, S., Tanihara, H., and Taga, T. (2006). *Activation of canonical Wnt pathway promotes proliferation of retinal stem cells derived from adult mouse ciliary margin.* Stem Cells 24 : 95-104.

Iozzo, R.V. (1997). *The family of the small leucine-rich proteoglycans: key regulators of matrix assembly and cellular growth.* Crit Rev Biochem Mol Biol 32: 141-174.

Islam, M.S. Shinmyo, Y. Okafuji, T. Su, Y. Naser, B.I. Ahmed, G. Zhang, S. Chen, S. Ohta, K. Kiyonari, H. Abe, T. Tanaka, S. Nishinakamura, R. Terashima, T. Kitamura, T. Tanaka, H. (2009) *Draxin, a repulsive guidance protein for spinal cord and forebrain commissures.* Science 323: 388-393.

Jouandet, M.L., Hartenstein, V., (1983) *Basal telencephalic origins of the anterior commissure of the rat*, Exp Brain Res 50 183-192.

Kaplan, M.S., Hinds.J. W.,(1977). *Neurogenesis in the adult rat : electron microscopic analysis of light radioautographs*. Science. 197: 1092-1094.

Keeble,T.R. Cooper, H.M. (2006) *Ryk: a novel Wnt receptor regulating axon pathfinding*, Int J Biochem Cell Biol 38: 2011-2017.

Kubo F., Takeichi M, & Nakagawa S (2005) *Wnt2b inhibits differentiation of retinal progenitor cells in the absence of Notch activity by downregulating the expression of proneural genes*. Development 132(12):2759-2770.

Kuriyama, S., Lupo, G, Ohta, K., Ohnuma, S., Harris, A.W., Tanaka, H., (2006). *Tsukushi controls ectodermal patterning and neural crest specification in Xenopus by direct regulation of BMP4 and X-delta-1 activity*. Development. 133: 75-88.

Lent, R. Uziel, D. Baudrimont, M. Fallet, C. (2005) *Cellular and molecular tunnels surrounding the forebrain commissures of human fetuses*. J Comp Neurol 483: 375-382.

Lindwall, C. Fothergill,T. Richards, J.L. (2007) *Commissure formation in the mammalian forebrain*. Curr Opin Neurobiol 17: 3-14.

Liu, H., Mohamed, O., Dufort, D., and Wallace, V.A. (2003). *Characterization of Wnt signaling components and activation of the Wnt canonical pathway in the murine retina*. Dev Dyn 227: 323-334.

Liu, H., Thurig, S., Mohamed, O., Dufort, D., and Wallace, V.A. (2006). *Mapping canonical Wnt signaling in the developing and adult retina*. Invest Ophthalmol Vis Sci 47: 5088-5097.

Liu, H., Xu, S., Wang, Y., Mazerolle, C., Thurig, S., Coles, B.L., Ren, J.C., Taketo, M.M., van der Kooy, D., and Wallace, V.A. (2007). *Ciliary margin transdifferentiation from neural retina is controlled by canonical Wnt signaling*. Dev Biol 308: 54-67.

Lord-Grignon, J., Abdouh, M., and Bernier, G. (2006). *Identification of genes expressed in retinal progenitor/stem cell colonies isolated from the ocular ciliary body of adult mice*. Gene Expr Patterns 6: 992-999.

Lozzo, R (1999). *The Biology of the Small Leucine-rich Proteoglycans*. The Journal of Biological Chemistry. 274: 18843-18846.

Martinez-Navarrete, G.C., Angulo, A., Martin-Nieto, J., and Cuenca, N. (2008). *Gradual morphogenesis of retinal neurons in the peripheral retinal margin of adult monkeys and humans*. J Comp Neurol 511 : 557-580.

Morris, A.S., Almeida, D.A., Tanaka, H., Ohta, K., Ohnuma, S., (2007). *Tsukushi modulates Xnr2, FGF and BMP signaling: regulation of Xenopus germ layer formation*. PLoS ONE 2: e1004.

Murata, T., Furushima, K., Hirano, M., Kiyonari, H., Nakamura, M., Suda, Y., and Aizawa, S. (2004). *Ang is a novel gene expressed in early neuroectoderm, but its null mutant exhibits no obvious phenotype*. Gene Expr Patterns 5: 171-178.

Ohta, K., Lupo, G., Kuriyama, S., Keynes, R., Holt, E. C., Harris, A. W., Tanaka, H., Ohnuma, S. (2004). *Tsukushi functions as an organizer inducer by inhibition of BMP activity in cooperation with chordin*. Dev Cell. 7: 347-358.

Ohta, K., Kuriyama, S., Okafuji, T., Gejima, R., Ohnuma, S., Tanaka, H., (2006). *Tsukushi cooperates with VGL1 to induce primitive streak and Hensen's node formation in the chick embryo*, Development. 133: 3777-3786.

Okafuji T & Tanaka H (2005) *Expression pattern of LINGO-1 in the developing nervous system of the chick embryo*. Gene Expr Patterns. 6:57-62.

Serafini, T. Colamarino, S.A. Leonardo, E.D. Wang, H. Beddington, R. Skarnes, W.C. Tessier-Lavigne, M. (1996) *Netrin-1 is required for commissural axon guidance in the developing vertebrate nervous system*. Cell 87: 1001-1014.

Schaefer, L. and Iozzo, R. (2008). *Biological Functions of the Small Leucine-rich Proteoglycans: From Genetics to Signal Transduction*. The Journal of Biological Chemistry. 283: 21305-21309.

Tole, S. Gutin, G. Bhatnagar, L. Remedios, R. Hebert, M.J. (2006) *Development of midline cell types and commissural axon tracts requires Fgfr1 in the cerebrum*. Dev Biol 289: 141-151.

Tropepe, V., Coles, B.L., Chiasson, B.J., Horsford, D.J., Elia, A.J., McInnes, R.R., and van der Kooy, D. (2000). *Retinal stem cells in the adult mammalian eye*. Science 287: 2032-2036.

Uemura, M. Takeichi, M. (2006) *Alpha N-catenin deficiency causes defects in axon migration and nuclear organization in restricted regions of the mouse brain*. Dev Dyn.

235: 2559-2566.

Van Raay, T.J., and Vetter, M.L. (2004). *Wnt/frizzled signaling during vertebrate retinal development*. Dev Neurosci 26: 352-358.

Viti, J. Gulacsi, A. Lillien, L. (2003) *Wnt regulation of progenitor maturation in the cortex depends on Shh or fibroblast growth factor 2*. J Neurosci 23: 5919-5927.

Xu, Q., Wang, Y., Dabdoub, A., Smallwood, P.M., Williams, J., Woods, C., Kelley, M.W., Jiang, L., Tasman, W., Zhang, K., *et al.* (2004). *Vascular development in the retina and inner ear: control by Norrin and Frizzled-4, a high-affinity ligand-receptor pair*. Cell 116: 883-895.

Yagi, T., Tokunaga, T., Furuta, Y., Nada, S., Yoshida, M., Tsukada, T., Saga, Y., Takeda, N., Ikawa, Y., and Aizawa, S. (1993). *A novel ES cell line, TT2, with high germline-differentiating potency*. Anal Biochem 214: 70-76.